A Hybrid Model to Study How Late Long Term Potentiation Is Affected by Faulty Molecules in an Intraneuronal Signaling Network Regulating Transcription Factor CREB

Ali Emadi[1 ‡], Mustafa Ozen[3,1 ‡], and Ali Abdi[1,2 *]

Ali Emadi
[1] Center for Wireless Information Processing
Dept. Electrical & Computer Engineering
New Jersey Institute of Technology (NJIT), Newark, NJ 07102, USA
Email: ae378@njit.edu

Mustafa Ozen
[3] Current Affiliation: Dept. of Biochemistry
Vanderbilt University, Nashville, TN 37240, USA
[1] Former Affiliation: Center for Wireless Information Processing, Dept. Electrical & Computer Engineering
New Jersey Institute of Technology (NJIT), Newark, NJ 07102, USA
Email: mustafa.ozen@vanderbilt.edu

Ali Abdi
[1] Center for Wireless Information Processing, Dept. Electrical & Computer Engineering
[2] Dept. of Biological Sciences
New Jersey Institute of Technology (NJIT), Newark, NJ 07102, USA
Email: ali.abdi@njit.edu
* Corresponding Author: Ali Abdi (ali.abdi@njit.edu)

‡ Contributed Equally

This is a pre-copyedited, author-produced version of an article accepted for publication in Integrative Biology following peer review. The version of record

A. Emadi, M. Ozen and A. Abdi, "A hybrid model to study how late long term potentiation is affected by faulty molecules in an intraneuronal signaling network regulating transcription factor CREB," Integrative Biology, vol. 14, pp. 111-125, 2022

is available online at: https://academic.oup.com/ib/article-abstract/14/5/111/6651319?redirectedFrom=fulltext
DOI: 10.1093/intbio/zyac011.

ABSTRACT

Systems biology analysis of intracellular signaling networks has tremendously expanded our understanding of normal and diseased cell behaviors and has revealed paths to finding proper therapeutic molecular targets. When it comes to neurons in the human brain, analysis of intraneuronal signaling networks provides invaluable information on learning, memory, and cognition related disorders, as well as potential therapeutic targets. However, neurons in the human brain form a highly complex neural network that, among its many roles, is also responsible for learning, memory formation, and cognition. Given the impairment of these processes in mental and psychiatric disorders, one can envision that analyzing interneuronal processes, together with analyzing intraneuronal signaling networks, can result in a better understanding of the pathology and, subsequently, more effective target discovery. In this paper, a hybrid model is introduced, composed of the long term potentiation (LTP) interneuronal process and an intraneuronal signaling network regulating CREB. LTP refers to an increased synaptic strength over a long period of time among neurons, typically induced upon occurring an activity that generates high frequency stimulations in the brain, and CREB is a transcription factor known to be highly involved in important functions of the cognitive and executive human brain such as learning and memory. The hybrid LTP-signaling model is analyzed using a proposed molecular fault diagnosis method. It allows to study the importance of various signaling molecules according to how much they affect an intercellular phenomenon when they are faulty, i.e., dysfunctional. This paper is intended to suggest another angle for understanding the pathology and therapeutic target discovery by classifying and ranking various intraneuronal signaling molecules based on how much their faulty behaviors affect an interneuronal process. Possible relations between the introduced hybrid analysis and the previous purely intracellular analysis are investigated in the paper as well.

STATEMENT OF INTEGRATION, INNOVATION, AND INSIGHT

Analysis of intracellular signaling networks using computational and systems biology approaches has expanded our understanding of normal and pathological cell behaviors. Integrated study of intercellular processes, together with intracellular signaling, is a promising hybrid approach that can add another dimension to our biological understanding. Here an inter-intracellular system is analyzed using a proposed hybrid molecular fault diagnosis method, which allows to study the importance of various signaling molecules based on how much they affect an intercellular phenomenon when they are faulty, i.e., dysfunctional. The integrated approach suggests another angle to better understand the pathology and advance therapeutic target discovery efforts.

INTRODUCTION

Signaling molecules are regulatory molecules, mostly enzymes, and receptors, involved in regulating many aspects of neuronal and cellular functions. Their dysfunction is known to contribute to the development of the pathology [1]. They have emerged as targets for developing new therapeutics [2], e.g., small molecules or other chemical entities that can control their activities.

There are a number of complex mental and psychiatric disorders, however, whose underlying molecular mechanisms are not well understood. Examples include schizophrenia, bipolar disorder, depression, etc. While a number of molecules are observed to be involved in such disorders, their roles and significance in the development of the pathology are not known. As a result, target discovery and drug development for effective treatment of such complex disorders have been highly challenging.

Systems biology approaches have been developed for finding therapeutic molecular targets, by analyzing intracellular signaling networks [3, 4][1]. In such approaches, first, a signaling network relevant to the disease of interest and regulates an important protein or transcription factor - called the output molecule - is considered. Then, several molecules are suggested as proper therapeutic candidates by analyzing some characteristics of the network and investigating certain functional relationships between the network output and the network components. As an example, see [8], where the focus is on leukemia.

[1] Other types of systems biology network analysis approaches address other subject matters, e.g., signaling network decision making [5], fitting a signaling network to experimental data [6], understanding gene regulatory networks [7], etc.

When it comes to mental and psychiatric disorders, naturally, one can similarly look at intraneuronal signaling networks. By analyzing signaling networks in neurons, one can find some possible therapeutic targets. However, neurons in the human brain form a highly complex neural network that is also responsible for learning, memory formation, and cognition, among its many roles. Given the impairment of these processes in mental and psychiatric disorders, one can envision that developing methodologies and tools to analyze interneuronal processes coupled with the intraneuronal signaling networks, can result in a better understanding of the pathology and, subsequently, more effective target discovery.

The interneuronal process considered in this paper, to be analyzed together with intraneuronal signaling, is the long term potentiation (LTP), discovered in 1973 [9]. LTP refers to an increased synaptic strength over a long period of time among neurons, typically induced upon occurring an activity that generates high frequency stimulations in the brain. Over the past few decades, extensive research has been conducted on various aspects of LTP [10], ranging from physiological mechanisms to learning and memory storage. Possible involvement of LTP and synaptic plasticity and their impairments in cognitive disorders such as schizophrenia and several others are also investigated by many groups of researchers [11, 12].

This paper introduces a hybrid model composed of the LTP and an intraneuronal signaling network regulating CREB, which is a slightly smaller copy of our previously studied CREB network [4] on which the used model is experimentally verified via Western blot analysis of protein extracts from primary neuronal cultures at multiple time points after treatment with different neurotransmitter ligands, and immunofluorescence analysis of primary cortical culture. CREB is a transcription factor known to be highly involved in essential functions of the cognitive and executive human brain, such as learning and memory. The hybrid LTP-signaling model is analyzed in this paper using a proposed molecular fault diagnosis method. It allows studying the importance of various signaling molecules according to how much they affect an intercellular phenomenon when they are faulty, i.e., dysfunctional. The paper is intended to suggest another angle for understanding the pathology and therapeutic target discovery, by classifying and ranking various intraneuronal signaling molecules based on how much their faulty behaviors affect an interneuronal process.

The rest of this paper is organized as follows. The first section introduces the hybrid LTP-signaling model, and its molecular fault diagnosis concepts are explained using two examples. Afterward, all the findings are presented and discussed in the RESULTS AND DISCUSSION section, followed by the METHODS and CONCLUSION sections.

THE HYBRID LTP-SIGNALING MODEL AND ITS FAULT DIAGNOSIS

A. The Hybrid LTP-Signaling Model

A schematic of the introduced neuronal hybrid LTP-signaling model is shown in Figure 1, in which a neuron generates electrical spikes in response to its input electrical spikes. Upon receiving certain high frequency spikes, neuronal activity and synaptic weight of the neuron - both to be defined later - can increase, which result in the long term potentiation. The magnitude of the LTP depends on the input stimulation, as well as the activity level of the transcription factor CREB in the neuron, regulated by an intraneuronal signaling network whose inputs are the important neurotransmitters acetylcholine, dopamine, serotonin, adenosine, and glutamate, and whose output is CREB. CREB is a cAMP response element-binding protein, where cAMP stands for cyclic adenosine monophosphate. In the rest of this subsection, first the signaling and then the LTP aspects of the hybrid model are introduced.

In general, each neuron in the human brain comprises many molecules that constantly interact with each other. These molecules constitute complex signaling networks that receive input signals from neurotransmitters and then generate responses that regulate some transcription factors, that can be considered as network outputs. Details of the intraneuronal signaling network considered in the hybrid model (Figure 1) are shown in Figure 2. The network is composed of five inputs - the neurotransmitters acetylcholine, dopamine, serotonin, adenosine, and glutamate, 51 intermediate molecules, 136 molecular interactions (Figure S1), and one output which is CREB (model simulation details and equations of the signaling network are provided in METHODS B). Studies in the nervous system of many organisms, from drosophila to vertebrate animals, have shown that a wide range of neurotransmitters, neuromodulators, and neurotrophic factors can control the transcriptional activities of numerous different genes co-regulated through a common cis-regulatory logic [13-19]. Such genes share a cis-regulatory motif, a DNA sequence in a locus of variable size, to which a transcription factor binds, affecting the locus's expression. There are hundreds of genes in neurons that have functional cis-regulatory elements (CREs). In neurons, CREB is known as the main regulator of the gene expression of such genes. The activity of CREB is induced in response to a variety of neurotransmitters, neuromodulators, and neurotrophic factors, which bind to their receptors and activate or inhibit several different classes of intraneuronal signaling molecules. A number of important physiological tasks of the central nervous system, such as memory formation, cognitive and

executive function, are regulated by changes in the expression or the activity of CRE responsive genes [13-19].

The LTP process in the hybrid model (Figure 1) includes the spike-timing-dependent plasticity (STDP) [20, 21] and the Bienenstock-Cooper-Munro (BCM) model of synaptic plasticity [22]. Basically, it is a simulation of late LTP in the hippocampal dentate gyrus, where the changing synaptic modification threshold, which specifies if the current activity of a neuron will make its input synapses stronger or weaker, depends on two parameters: average postsynaptic spike count of the neuron, and concentration of phosphorylated, i.e., activated CREB. Note that the activation of CREB induces gene expression that results in maintaining the late LTP. Equations and model simulation details for the LTP are provided in METHODS A.

The details of the hybrid LTP-signaling model, which is a combination of the STDP-BCM synaptic plasticity and the intraneuronal CREB signaling network, are provided in METHODS C.

All findings of the hybrid LTP-signaling model fault diagnosis, which is essentially an analysis from a pathology perspective, are presented in RESULTS AND DISCUSSION in detail. In the following subsection, nevertheless, two of the results are discussed to present key ideas and gain insight.

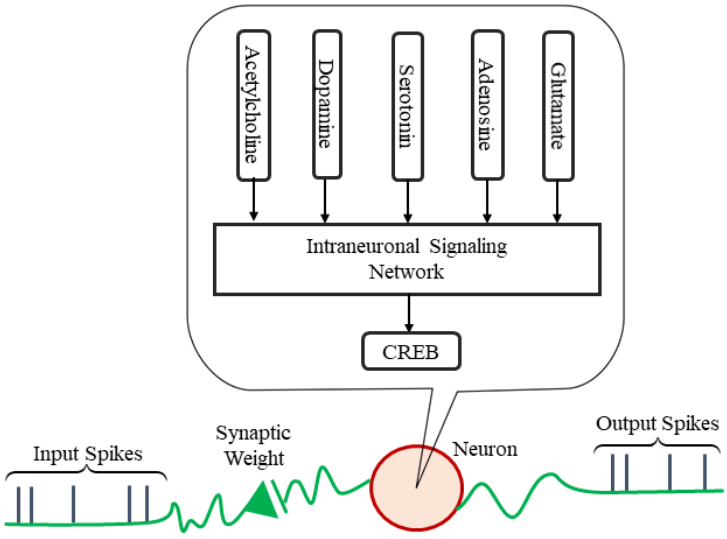

Figure 1. The introduced hybrid LTP-signaling model of a neuron that generates electrical spikes in response to its input electrical spikes. Upon receiving certain high frequency spikes, neuronal activity and synaptic weight of the neuron can increase, that result in long term potentiation. The magnitude of the long term potentiation depends on the input stimulation, as well as the activity level of the transcription factor CREB in the neuron, regulated by an intraneuronal signaling network whose inputs are the important neurotransmitters acetylcholine, dopamine, serotonin, adenosine, and glutamate.

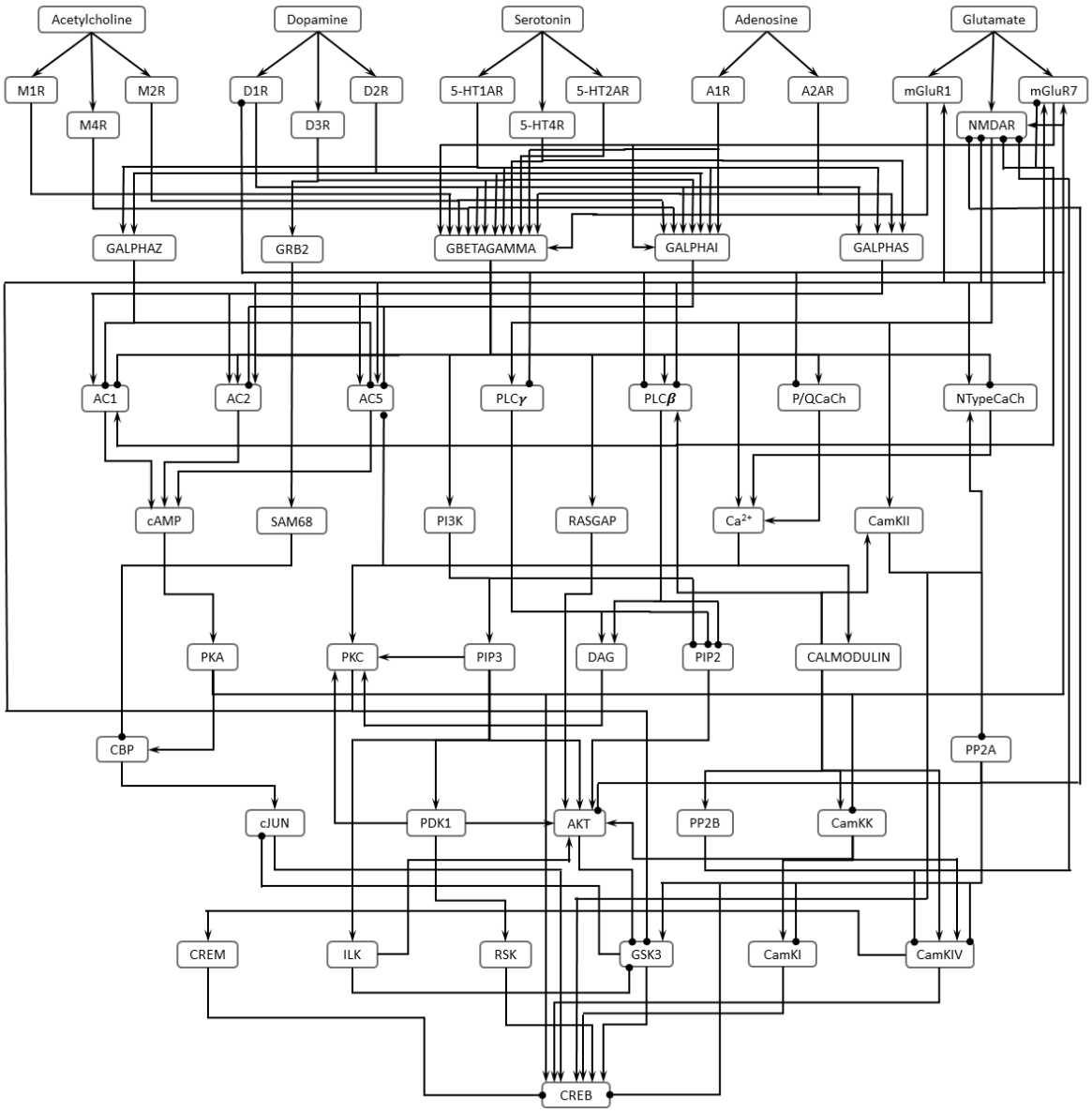

Figure 2. The CREB intraneuronal signaling network. The network has a total of 57 molecules. The inputs are the neurotransmitters acetylcholine, dopamine, serotonin, adenosine, and glutamate, and the output is the transcription factor CREB. The normal arrows represent activatory interactions whereas the circle-headed arrows represent inhibitory interactions.

B. Molecular Fault Diagnosis of the Hybrid LTP-Signaling Model: Two Examples

A principal goal of analyzing signaling networks is to understand how a physiological state is turned into a pathological state and what elements play critical roles in this transition. To understand why and how a signaling network fails, one needs to find out to what extent individual molecules or groups of molecules contribute to the breakdown of the network. This allows us to dissect out how numerous different

components of a variety of signaling pathways may contribute to the system failure when they become faulty, i.e., dysfunctional. In turn, this will tell us how much emphasis we should put on those molecules which are identified as major contributors in the stage of drug development.

In our prior studies, an experimentally-verified molecular fault diagnosis approach was developed [4, 23, and 24], to determine the most vulnerable molecules in a network of molecules. A high vulnerability for a molecule means that with high probability, the whole signaling network does not operate correctly if the molecule is faulty. Those studies focused on understanding the amount of departure of the signaling network response from its normal response, when there were faulty molecules in the network. This was a purely intracellular analysis, whereas this paper studies the importance of various signaling molecules according to how much they affect LTP - an intercellular phenomenon - when they are faulty. This study is intended to add another angle to understanding the pathology and therapeutic target discovery for cognition and memory-impaired complex mental disorders, by classifying and ranking various intraneuronal signaling molecules based on how much their faulty behaviors affect an interneuronal process. Possible relations between this hybrid approach and the previous analysis are discussed in RESULTS AND DISCUSSION as well.

Example 1: Based on our analysis, Figure 3A shows how two different molecules affect neuronal activity differently, when they are faulty (see METHODS for simulation details and equations). Following [20, 21], here the neuronal activity is considered as the moving time-average of postsynaptic spike count of a neuron, typically after receiving a high frequency stimulation (HFS). The red graph is the neuronal activity of a wild-type neuron that has received a 95 msec HFS at 2 h [20]. The other two graphs are simulation results of the hybrid model, when the signaling network (Figure 2) has one faulty molecule. It appears that a faulty CAMKK does not deviate the neuronal activity from the wild-type activity, whereas a faulty PKA considerably reduces the neuronal activity. The effects of all the molecules in the intraneuronal signaling network (Figure 2) on the neuronal activity, when they are faulty, are presented and discussed in RESULTS AND DISCUSSION.

Example 2: According to our analysis, Figure 3B demonstrates that if two molecules are concurrently faulty, their damaging impact on the neuronal activity can be more profound, compared to only one of them being faulty (see METHODS for simulation details and equations). The red graph is the neuronal activity of a wild-type neuron that has received HFS at 2 h [20]. The other three graphs are simulation results of the hybrid model, when the signaling network (Figure 2) has one or two faulty molecules. In this example, we observe that when either cAMP or CREM is faulty, the neuronal activity reduces with respect to the wild-type activity. However, when they are both faulty together, the neuronal

activity decreases further. The effects of all pairs of molecules in the intraneuronal signaling network (Figure 2) on the neuronal activity, when they are concurrently faulty, are presented and discussed in RESULTS AND DISCUSSION.

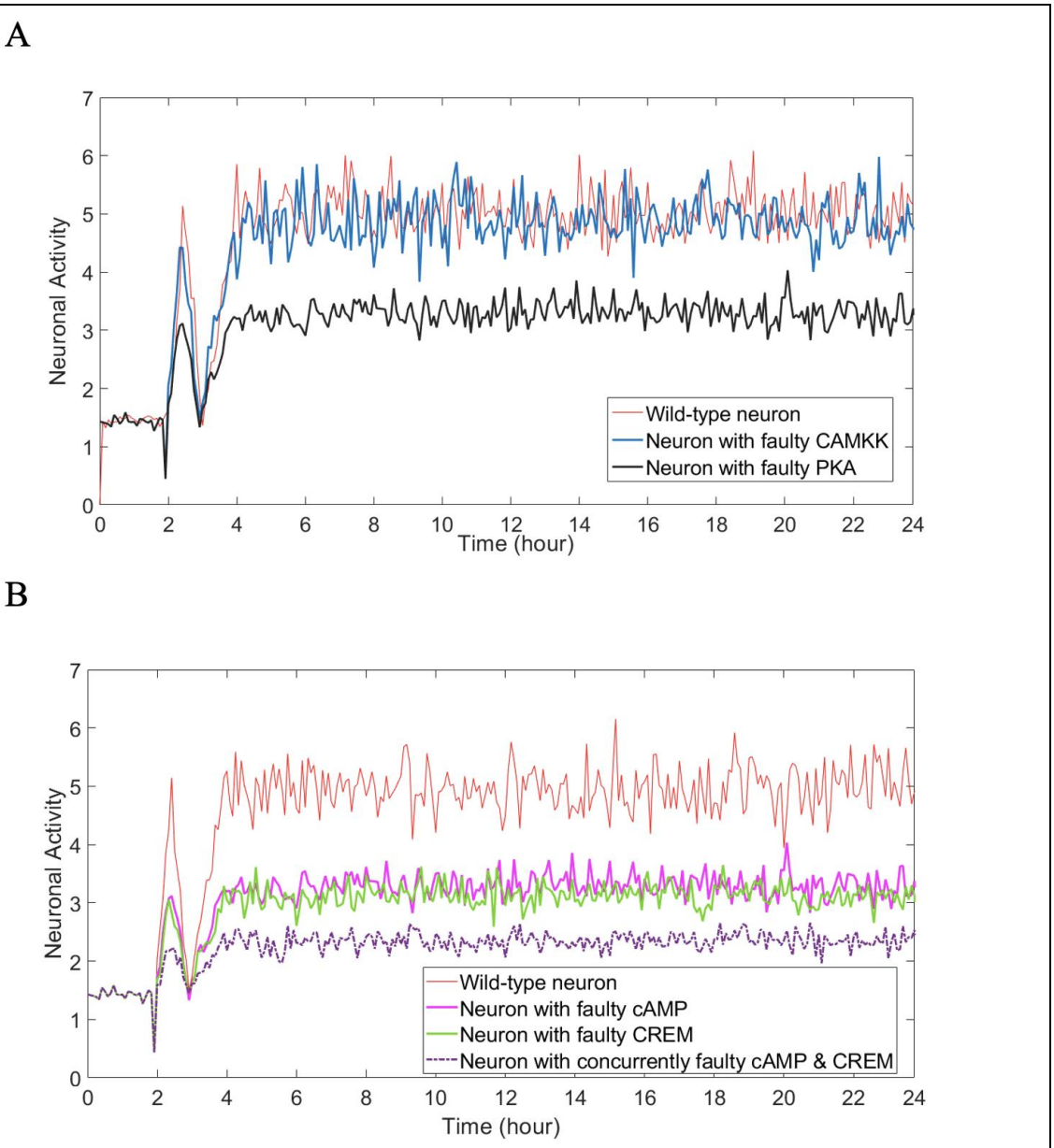

Figure 3. Examples of neuronal activity variations versus time when a high frequency stimulation is applied in 2 hours. **(A)** Example 1: Red: a wild-type neuron [20]; Blue: a neuron in which a molecule called CAMKK is faulty in the CREB signaling network; Black: a neuron in which a molecule called PKA is faulty in the CREB signaling network. **(B)** Example 2: Red: a wild-type neuron [20]; Magenta: a neuron in which a molecule called cAMP is faulty in the CREB signaling network; Green: a neuron in which a molecule called CREM is faulty in the CREB signaling network; Purple: a neuron in which the two molecules cAMP and CREM are concurrently faulty in the CREB signaling network.

RESULTS AND DISCUSSION

In this section, results of the fault diagnosis of the hybrid LTP-signaling model are presented using two important synaptic plasticity parameters: neuronal activity and synaptic weight. Following [20, 21], the neuronal activity is the moving time-average of postsynaptic spike count of a neuron after receiving HFS, whereas the synaptic weight represents the field excitatory post synaptic potential (fEPSP). The following two subsections, A and B, are dedicated to presenting the neuronal activity and the synaptic weight fault diagnosis results, respectively (see METHODS for simulation details and equations).

A. Neuronal Activity Results

Neuronal activity variations versus time, when a high frequency stimulation is applied to the neuron and there is one faulty molecule in the intraneuronal CREB signaling network, are shown in Figure 4A. Depending on the level of impact of the faulty molecule on CREB, molecules are categorized into seven classes (Figure S2A, Table S2). We observe that some classes are close to the wild-type neuron graph, whereas others exhibit noticeable deviations from it. To better understand this, neuronal activity averages are computed over 6-24 h steady-state time courses of Figure 4A, for each class of faulty molecules, as well as the wild-type neuron (Figure 4B). Averages of classes 1-3 are found to be close to the neuronal activity average of the wild-type neuron, assuming a +/-10% range as a measure of closeness, whereas noticeable differences are observed between the averages of classes 4-7 and the wild-type neuron average activity.

Additionally, variations in the neuronal activity are examined in the presence of two concurrently faulty molecules in the intraneuronal CREB signaling network, when a high frequency stimulation is applied to the neuron (Figure 5A). In this instance, pairs of molecules are categorized into twenty nine classes (Figure S2B, Table S3.1-S3.29), based on the level of impact of the faulty pair of molecules on CREB. While some of the classes are close to the wild-type neuron response, others exhibit noticeable deviations. Upon computing the neuronal activity averages over the 6-24 h steady-state time courses of Figure 5A for each class of faulty pairs of molecules, as well as the wild-type neuron, we observe that averages of classes 1-7 are close to the neuronal activity average of the wild-type, whereas averages of classes 8-29 are noticeably different, more than 10%, compared to the wild-type neuron average activity (Figure 5B).

The above results obtained from the analysis of the hybrid model demonstrate that depending on what molecule or pair of molecules is faulty in the CREB signaling network, then the HFS average neuronal activity can change slightly or considerably (Figures 4B and 5B). These results suggest different roles for

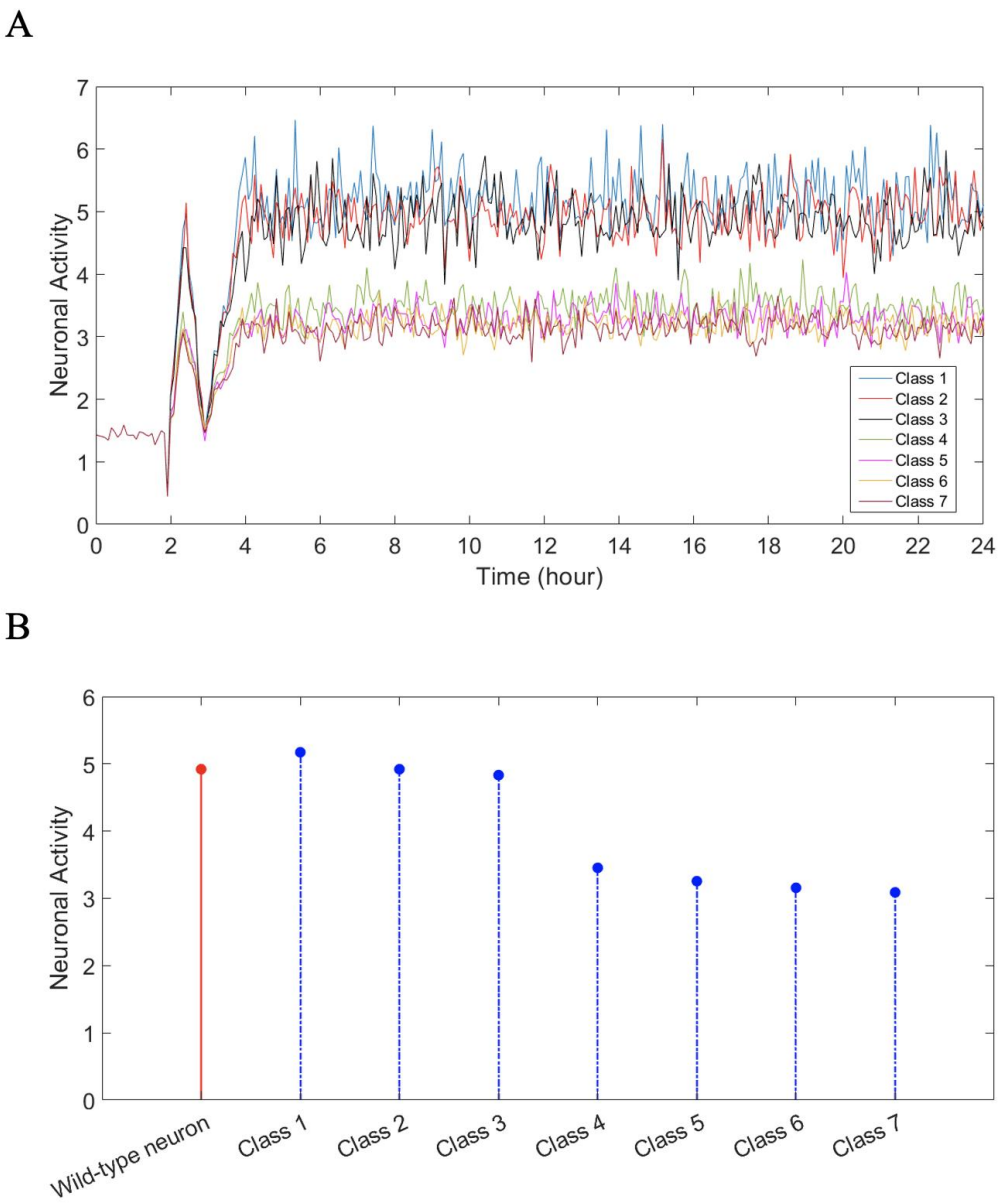

Figure 4. Neuronal activity analysis results when there is one faulty molecule in the intraneuronal CREB signaling network. **(A)** Neuronal activity variations versus time, when a high frequency stimulation is applied to the neuron. Depending on the level of impact of the faulty molecule on CREB, molecules are categorized to seven classes, and the corresponding neuronal activities are shown by different colors. The included wild-type neuronal activity graph (also shown in Figure 3B) is the same as class 2 graph. **(B)** Neuronal activity averages computed over the steady-state time courses of panel A, for each class of faulty molecules, as well as the wild-type neuron.

the signaling molecules, according to how much deviations from the wild-type HFS neuronal activity they induce, when they are faulty. It is informative to additionally investigate what the impacts of faculty molecules are, if they are studied from a pure intraneuronal signaling perspective, and not using the hybrid

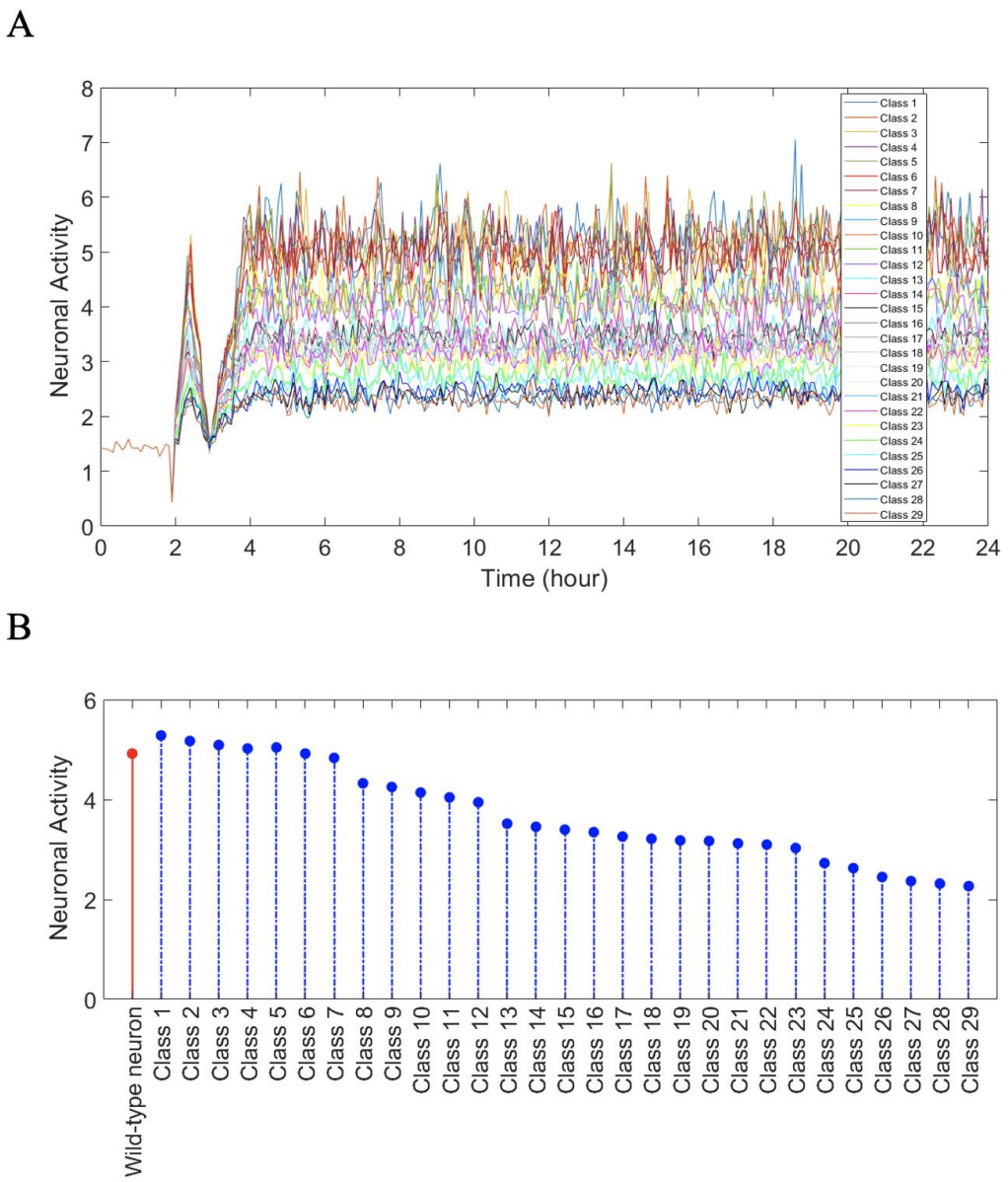

Figure 5. Neuronal activity analysis results when there are two concurrently faulty molecules in the intraneuronal CREB signaling network. **(A)** Neuronal activity variations versus time, when a high frequency stimulation is applied to the neuron. Depending on the level of impact of the faulty pair of molecules on CREB, pairs of molecules are categorized to twenty nine classes, and the corresponding neuronal activities are shown by various colors. The included wild-type neuronal activity graph (also shown in Figure 3B) is the same as the class 6 graph. **(B)** Neuronal activity averages computed over the steady-state time courses of panel A, for each class of faulty pairs of molecules, as well as the wild-type neuron.

approach. In our prior studies, an intracellular fault diagnosis approach was developed [4, 23, and 24], to find the most vulnerable molecules in a network of molecules. A high vulnerability for a molecule means that with high probability, the whole signaling network does not operate correctly, if the molecule is faulty.

The focus of those studies was on analyzing the amount of deviation of the signaling network response from its normal response, when there were faulty molecules in the network. This was a purely intracellular analysis, whereas this paper studies the importance of various signaling molecules according to how much they affect a combination of intercellular and intracellular processes, when the molecules are faulty.

To compare with the results of the hybrid analysis of this paper, vulnerability levels of all the 51 individual molecules (Figure S3A, Table S4) and all the 1275 pairs of molecules (Figure S3B, Table S5.1-S5.14) are computed for the intraneuronal CREB signaling network (Figure 2), when they are faulty (see METHODS B for details). We note that single-fault vulnerabilities change from 0 to 0.6, whereas double-fault vulnerabilities vary over a wider range of 0 to 0.8. This indicates that when two molecules are concurrently faulty, they may cause more harm to the signaling network, compared to being individually faulty.

To understand the relation between the hybrid and the pure intraneuronal analyses results and the way they rank single faulty molecules, normalized neuronal activity when there is one faulty molecule in the intraneuronal CREB signaling network, versus the vulnerability level of the faulty molecule, is depicted in a scatter plot (Figure 6A). Here the *normalized* neuronal activity for each class of molecules is obtained via dividing the class neuronal activity of Figure 4B by the neuronal activity of the wild-type neuron, whereas each vulnerability level is taken from Figure S3A. We observe that classes 1-3 whose normalized neuronal activities are close to 1 (close to the wild-type neuronal activity), exhibit low vulnerability levels, whereas classes 4-7 that have normalized neuronal activities far away from 1, demonstrate high vulnerability levels. This is an intuitively reasonable observation, as one expects that a faulty highly vulnerable molecule should impair the neuronal activity significantly, whereas a faulty molecule with low vulnerability should not induce noticeable deviation from the wild-type activity.

Similarly, a scatter plot is created using the normalized neuronal activity and the intraneuronal vulnerability levels, when there are two concurrently faulty molecules in the intraneuronal CREB signaling network. This allows to examine the hybrid and the pure intraneuronal approaches and understand how they rank double faulty molecules (Figure 6B, Table S6). The *normalized* neuronal activity for each class of molecule pairs is obtained via dividing the class neuronal activity of Figure 5B by the neuronal activity of the wild-type neuron, whereas each vulnerability level is taken from Figure S3B. We note that those classes whose normalized neuronal activities are close to 1 - close to the wild-type neuronal activity - exhibit low vulnerability levels, whereas classes that have normalized neuronal activities far away from 1, demonstrate high vulnerability levels. Similar to the single fault analysis, this is reasonable, as one anticipates that a

faulty highly vulnerable pair of molecules should affect the neuronal activity more. In contrast, a faulty pair of molecules with low vulnerability should not cause a major deviation from the wild-type activity.

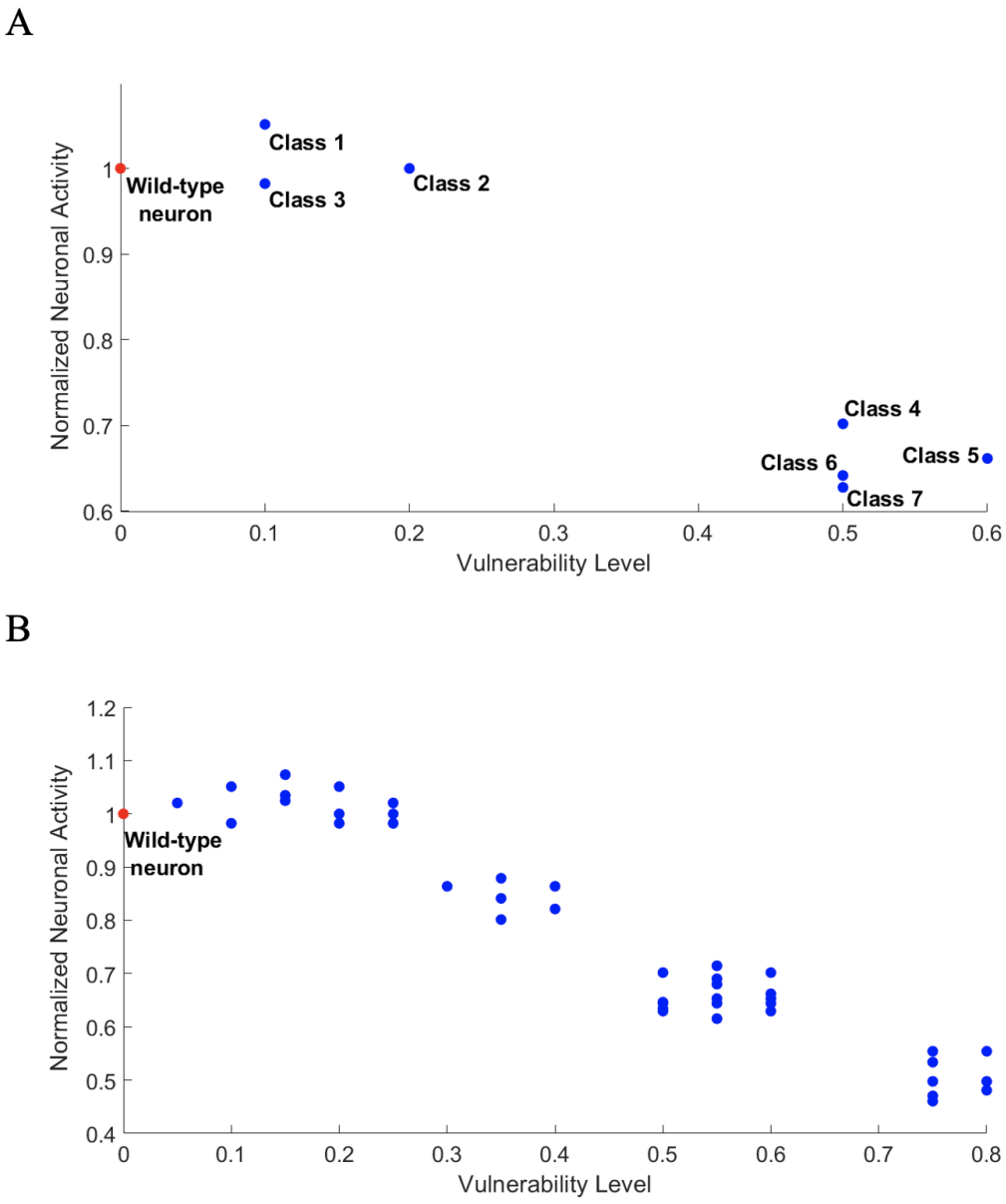

Figure 6. Normalized neuronal activity versus vulnerability levels. **(A)** Normalized neuronal activity when there is one faulty molecule in the intraneuronal CREB signaling network, versus the vulnerability level of the faulty molecule. Depending on the amount of impact of the faulty molecule on CREB, molecules are categorized to seven classes. **(B)** Normalized neuronal activity when there are two concurrently faulty molecules in the intraneuronal CREB signaling network, versus the vulnerability level of the faulty pair of molecules. Depending on the level of impact of the faulty pair of molecules on CREB, pairs of molecules are categorized to twenty nine classes. Table S6 specifies the class labels for the data points in the figure.

B. Synaptic Weight Results

In this subsection, results of the fault diagnosis of the hybrid LTP-signaling model are presented using the important synaptic plasticity parameter called synaptic weight [20, 21], which represents the induced field excitatory post synaptic potential, in response to the HFS of the perforant pathway [20] (see METHODS for simulation details and equations).

Here we examine variations in the synaptic weight versus time and in the presence of an individually faulty molecule (Figure S4A), or two concurrently faulty molecules (Figure S4B) in the intraneuronal CREB signaling network. Depending on the level of impact of the molecular dysfunctionalities on CREB, the individually faulty molecules are categorized into seven classes (Figure S2A, Table S2), whereas the pairs of faulty molecules are categorized into twenty nine classes (Figure S2B, Table S3.1-S3.29), where various classes can behave differently. Furthermore, using their respective 6-24 h steady-state time courses (Figure S4A and S4B), we compute the average synaptic weight for each class of individually faulty molecules (Figure 7A), as well as the concurrently faulty pairs of molecules (Figure 7B), and compare with the wild-type neuron. For the single fault case, averages of classes 2-3 are found to be close to the synaptic weight average of the wild-type neuron, assuming a +/-10% range as a measure of closeness, whereas noticeable differences are observed between the averages of other classes and the wild-type average synaptic weight. On the other hand, in the case of a concurrently faulty pair of molecules, averages of classes 3-8 are found to be close to the synaptic weight average of the wild-type neuron, whereas the rest of the classes exhibit more noticeable differences with respect to the wild-type average synaptic weight.

These analyses demonstrate that the HFS average synaptic weight can alter slightly or substantially (Figure 7), depending on what molecule or pair of molecules is faulty in the CREB signaling network. Moreover, these results suggest different roles for the signaling molecules, according to how much deviations from the wild-type HFS synaptic weight they induce, when they are faulty.

To understand the relation between the hybrid synaptic weight analysis and the pure intraneuronal vulnerability analysis results explained in the previous section (Figure S3), and how they rank individual and pairs of faulty molecules, now we generate two scatter plots. They show the normalized synaptic weight versus the vulnerability level when there is one faulty molecule (Figure 8A) or there are two concurrently faulty molecules (Figure 8B) in the intraneuronal CREB signaling network. The *normalized* synaptic weight for each class of molecules is obtained via dividing the associated synaptic weight by the synaptic weight of the wild-type neuron, whereas each vulnerability level is taken from Figure S3A and S3B for individual and pairs of faulty molecules, respectively. We observe that the molecules in classes 1-3 whose normalized

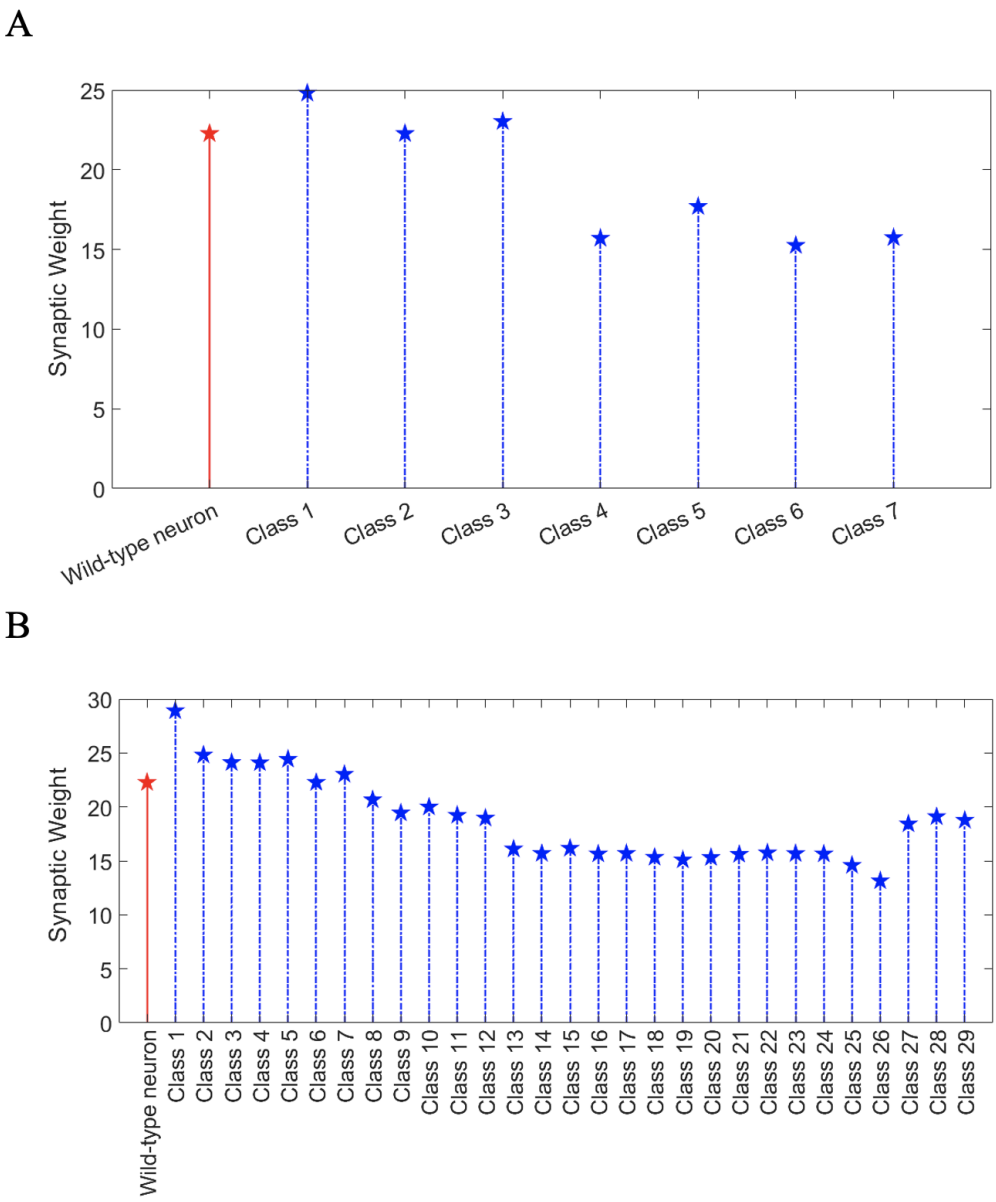

Figure 7. Synaptic weight averages computed over the steady-state time courses. **(A)** Synaptic weight averages computed over the steady-state time courses of Figure S4A, for each class of faulty molecules, as well as the wild-type neuron. **(B)** Synaptic weight averages computed over the steady-state time courses of Figure S4B, for each class of faulty pairs of molecules, as well as the wild-type neuron.

synaptic weights are close to 1, i.e., close to the wild-type synaptic weight, exhibit low individual vulnerability levels, whereas the molecules of classes 4-7 that have normalized synaptic weights distant from 1, show high individual vulnerability levels (Figure 8A). We also observe that the normalized synaptic weight typically decreases, as the vulnerability level increases in the presence of two concurrently faulty molecules (Figure 8B). This is intuitively reasonable, as one expects that faulty highly vulnerable

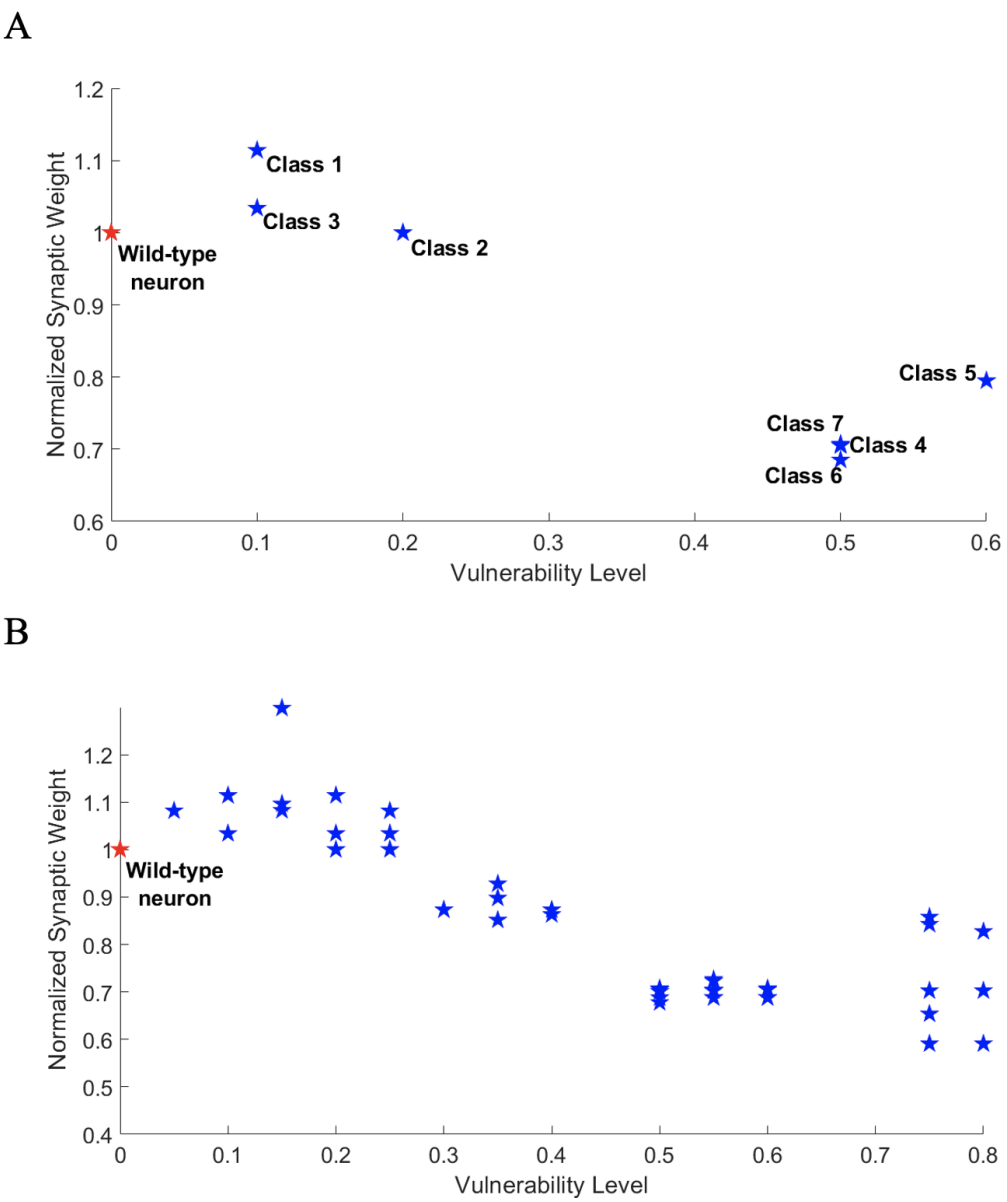

Figure 8. Normalized synaptic weight versus vulnerability levels. **(A)** Normalized synaptic weight when there is one faulty molecule in the intraneuronal CREB signaling network, versus the vulnerability level of the faulty molecule. Depending on the amount of impact of the faulty molecule on CREB, molecules are categorized to seven classes. **(B)** Normalized synaptic weight when there are two concurrently faulty molecules in the intraneuronal CREB signaling network, versus the vulnerability level of the faulty pair of molecules. Depending on the level of impact of the faulty pair of molecules on CREB, pairs of molecules are categorized to twenty nine classes. Table S7 specifies the class labels for the data points in the figure.

molecule(s) should impair the synaptic weight significantly, whereas faulty molecule(s) with low vulnerability should not cause substantial deviation from the wild-type synaptic weight.

Interestingly, there are some additional lessons that we can learn from Figure 8B, which can be useful for therapeutic target discovery. For example, the three star markers at the lower right corner of Figure 8B represent three distinct sets of molecular pairs with the same highest vulnerability of 0.8. More specifically and according to Table S5.1, there are the following 34 such pairs with equal vulnerability of 0.8: PKA-PP2B, PKA-CAMKIV, PKA-CREM, CALMODULIN-PP2B, CALMODULIN-CAMKIV, CALMODULIN-CREM, PP2A-PP2B, PP2A-CAMKIV, PP2A-CREM, PP2B-GALPHAI, PP2B-PQCaCh, PP2B-CAMKII, PP2B-CALCIUM, PP2B-AC2, PP2B-cAMP, GALPHAI-GBETAGAMMA, GALPHAI-AC1, GALPHAI-AC5, GALPHAI-CAMKIV, GALPHAI-CREM, GBETAGAMMA-AC2, GBETAGAMMA-cAMP, PQCaCh-CREM, PQCaCh-CAMKIV, CAMKII-CAMKIV, CAMKII-CREM, CALCIUM-CAMKIV, CALCIUM-CREM, AC1-AC2, AC5-AC2, AC2-CAMKIV, AC2-CREM, cAMP-CAMKIV, cAMP-CREM.

In general, it may not be straightforward to decide what the best pair of molecules is to choose for therapeutic targeting, given the above large number of choices with the same vulnerability level. Upon looking at Figure 8B, however, we find out that there are three different normalized synaptic weights associated with the above pairs, when they are faulty: 0.827, 0.703, and 0.591 (which correspond to classes 27, 24, and 26, respectively, according to Table S7). Note that the pairs with the normalized synaptic weight of 0.591 in Figure 8B exhibit the largest deviation from the wild-type synaptic weight, when they are faulty. Subsequently, one may say that such pairs with the highest vulnerability of 0.8 are more likely to contribute more to the development of the pathology, when they become dysfunctional. Therefore, such pairs are probably better targets for drug development and delivery, compared to other pairs of molecules that have the same high vulnerability of 0.8. This example demonstrates how the introduced hybrid approach can add another dimension to intraneuronal signaling-based target discovery methods.

METHODS

A. The Neuron Model, Spike-Timing-Dependent Plasticity (STDP), Bienenstock-Cooper-Munro (BCM) Synaptic Plasticity Model, and CREB

Our spiking model for a hippocampal dentate granule cell has two excitatory inputs representing ipsilateral medial and ipsilateral lateral perforant pathways, mpp and lpp, respectively. The pathway shown in Figure 1 is the ipsilateral perforant pathway, pp, which is the mixture of mpp and lpp [20].

The Izhikevich model used as our neuron model in Figure 1 is composed of the following two ordinary differential equations [25]:

$$\frac{dv(t)}{dt} = 0.04v^2(t) + 5v(t) + 140 - u(t) + I(t), \tag{1}$$

$$\frac{du(t)}{dt} = a(bv(t) - u(t)), \tag{2}$$

where $v(t)$, a dimensionless variable, is the neuron membrane potential, $u(t)$ represents the membrane recovery variable that applies a negative feedback to $v(t)$, to incorporate the inactivation and activation of the Na^+ and K^+ ionic currents, respectively, $I(t)$ is the variable that delivers synaptic inputs, $a = 0.02$ and $b = 0.2$. The model works as follows:

$$\text{If } v(t) \geq \text{AP}, \quad \text{then} \begin{cases} v(t) \leftarrow c, \\ u(t) \leftarrow u(t) + d. \end{cases} \tag{3}$$

This means that when the membrane potential reaches its apex value of $\text{AP} = 55\,\text{mV}$, then $v(t)$ and $u(t)$ are updated following Equation (3), where $c = -69$ mV, $d = 2$, and time step and spike width in simulations are 1 ms. The total synaptic input of the model $I(t)$ due to separate input pathways is given by [20]:

$$I(t) = h(t)I_{mpp}w_{mpp}(t) + h(t)I_{lpp}w_{lpp}(t), \tag{4}$$

where $h(t) = 1$ or 0, whenever a presynaptic spike exists or not at the time instant *t*, $I_{mpp} = I_{lpp} = 100$ are the intensities of electrical stimulation of the mpp and lpp pathways, respectively, and $w_{mpp}(t)$ and $w_{lpp}(t)$ are the weights of the mpp and lpp inputs, respectively. Initial weight of each pathway is considered to 0.05.

In our simulations, spontaneous input spikes are a superposition of an 8 Hz correlated component and a 1 Hz uncorrelated component composed of Poisson random spikes [20]. To trigger late long term potentiation (LTP), high frequency stimulation (HFS) is injected into the perforant pathway pp, following the protocol of [20], shown in Figure S5.

STDP is a temporally asymmetric type of Hebbian rule, induced by temporal correlation of presynaptic and postsynaptic spikes. Both spontaneous spikes and HFS inputs are considered for implementing STDP. Additionally, the nearest-neighbor rule is used to implement STDP, i.e., each presynaptic spike can pair with just two postsynaptic spikes: one appearing immediately before and one appearing immediately after the said presynaptic spike. More specifically, synaptic weight changes and update are given by the following equations [20, 26]:

$$\Delta w_+(\Delta t) = A_+(t)\exp(-\Delta t/\tau_+), \quad \text{if } \Delta t > 0, \tag{5}$$

$$\Delta w_-(\Delta t) = A_-(t)\exp(\Delta t/\tau_-), \quad \text{if } \Delta t < 0, \tag{6}$$

$$w(t+\delta t) = w(t)(1+\Delta w_+ - \Delta w_-), \tag{7}$$

where $\Delta t = t_{post} - t_{pre}$, $\tau_+ = 10$ ms and $\tau_- = 100$ ms are the post and presynaptic spikes time difference, synaptic potentiation modification window and synaptic depression modification window, respectively, and weight update occurs every $\delta t = 1$ ms. Additionally, $A_+(t)$ and $A_-(t)$ are amplitudes for the positive (potentiation) and negative (depression) synaptic changes, respectively, defined by the following equations:

$$A_+(t) = A_+(0)/\theta_M(t), \tag{8}$$

$$A_-(t) = A_-(0)\theta_M(t), \tag{9}$$

where $A_+(0) = 0.02$ and $A_-(0) = 0.01$ are initial synaptic potentiation and depression amplitudes, respectively, and $\theta_M(t)$ is the time-varying LTP threshold coming from the BCM theory [22], and determines the direction of synaptic plasticity and the easiness of LTP induction. It is considered to be a function of both postsynaptic and CREB activities [20]:

$$\theta_M(t) = \alpha F_1(t)F_2(t), \tag{10}$$

where $\alpha = 2000$ is a scaling factor and $F_1(t)$ is the time-average of postsynaptic spikes over the most recent window of length $\tau_M = 30$ s:

$$F_1(t) = \tau_M^{-1}\int_{-\infty}^{t} c(t')\exp\left(-(t-t')/\tau_M\right)dt', \tag{11}$$

where $c(t') = 1$ or 0, if a postsynaptic spike at the time t' exists or not, respectively (Note that the time-varying "neuronal activity" discussed and graphed in the figures of the main body of the paper is indeed

$\alpha F_1(t)$). Moreover, $F_2(t)$ is the inverse of the phosphorylated CREB concentration in the postsynaptic neuron $[\text{pCREB}(t)]$, which is a measure of CREB activity:

$$F_2(t) = 1/[\text{pCREB}(t)]. \tag{12}$$

As mentioned at the beginning of RESULTS AND DISCUSSION and used in the figures and discussions in the main body of the paper, the term "synaptic weight" is used to represent the experimentally-important quantity called field excitatory post synaptic potential (fEPSP). More specifically, all the "synaptic weight" figures and results in the paper are generated using Equation (13) below, which is the fEPSP percentage change response to the stimulation of the perforant pathway pp, computed based on the linear summation of the percentage changes of the medial and lateral perforant pathways mpp and lpp weights:

$$\Delta\text{fEPSP}_{pp}(t)\% = \Delta w_{mpp}(t)\% + \Delta w_{lpp}(t)\%, \tag{13}$$

$$\Delta w_{mpp}(t)\% = 100\left(\frac{w_{mpp}(t) - w_{mpp}(0)}{w_{mpp}(0)}\right), \quad w_{mpp}(0) = 0.05, \tag{14}$$

$$\Delta w_{lpp}(t)\% = 100\left(\frac{w_{lpp}(t) - w_{lpp}(0)}{w_{lpp}(0)}\right), \quad w_{lpp}(0) = 0.05, \tag{15}$$

where $w_{mpp}(t)$ and $w_{lpp}(t)$ are computed using Equation (7).

At the end, note that all the "neuronal activity" and "synaptic weight" figures and results are obtained by generating and averaging over six realizations of $\alpha F_1(t)$ and $\Delta\text{fEPSP}_{pp}(t)\%$, respectively.

B. The Intraneuronal CREB Signaling Network

We use the discrete modeling approach to model and simulate the intraneuronal CREB signaling network (Figure 2) [27]. It is advantageous for signaling networks with many molecular interactions, whose mechanistic details, kinetic parameters, rate constants, etc., are not available. This approach is used by various groups of researchers, e.g., [3-8]. The discrete modeling approach and the CREB network were already experimentally verified using Western blot and immunofluorescence analyses (see [4] for details).

To simulate the CREB activity level using the regulatory equations of the network molecules of Figure 2 listed in Table S1, we follow the approach provided in [5]. To elaborate, the CREB activity level is computed by simulating the CREB network for 1000 iterations, when one input molecule is active at a time. The percentage of CREB being the binary 1 in the last 100 iterations - when the network reaches the steady state - specifies the CREB activity level [5] for that specific input. We repeat this for all the input

molecules and then average over the computed CREB activity levels, which provides the overall CREB activity level for the five input molecules. This quantity is called $CREB_{network}$, which is a measure of the CREB activity level induced by the CREB intraneuronal signaling network.

We compute the CREB activity level $CREB_{network}$ for both normal and abnormal networks, in which one or two molecules are considered to be faulty, i.e., dysfunctional. The faulty state of a molecule can be defined as its failure to respond correctly to the input signals, which can ultimately induce incorrect responses at the output of the network and change the output activity accordingly. To model a faulty molecule, we consider that its activity state is either stuck-at-0, sa0, or stuck-at-1, sa1, each with a probability of 1/2 [4]. Similarly, when there exist two concurrently faulty molecules in the network, we consider that each molecule in the faulty pair is equi-probably sa0 or sa1. The $CREB_{network}$ activity values with no, one, and two faulty molecules in the signaling network are provided in Figure S2A and S2B, respectively, after a numerical scaling explained in METHODS C (see Equation (19)). The results are also listed in Table S2 and Table S3, respectively.

To compare the results of the hybrid analysis of this paper with a purely intracellular analysis, we compute the vulnerability level of each molecule, and each pair of molecules, as follows [4, 23]: First, we simulate the fault-free (normal) network for 1000 iterations for each input being active at a time and observe the fault-free responses at the network output CREB. Then, we simulate the abnormal network for 1000 iterations, where a specific molecule or a specific pair of molecules is rendered faulty, such that each faulty activity state is either sa0 or sa1 with a probability of 1/2 [4], and observe the faulty network CREB responses for each input being active at a time. Afterward, we compare the abnormal and normal network CREB responses in the last 100 iterations [5], to compute the probability of having incorrect network responses. This is the vulnerability level of that specific molecule or pair of molecules. Mathematical details of computing single and double fault vulnerability levels are given below.

Recall that the intraneuronal CREB signaling network has one output and 5 inputs, and the network responses in the last 100 iterations [5], i.e., after reaching the steady state, are considered to compute the vulnerability levels for single and double fault analyses. This means that in the presences of a faulty molecule (or two concurrently faulty molecules) and for each input being active at a time, there will be 100 output responses that may be the same as or different from the 100 normal network responses. Suppose that β_i is the vector of responses of the normal network and γ_i is the vector of responses of the abnormal network - in which there exists a single or a pair of faulty molecules - in the last 100 iterations, when the input i is active, $i = 1,...,5$. To compute the vulnerability level, one needs to compare β_i with γ_i for each i and in the presence of a specific faulty molecule (or a pair of concurrently faulty molecules):

$$\varepsilon_i = \beta_i - \gamma_i . \tag{16}$$

Here ε_i is either a vector of all zeros represented by **0**, if there is not any incorrect network response, or it contains at least one non-zero entry, if there exists at least one incorrect network response in any of the 100 iterations.

When a single molecule *x* is faulty, the vulnerability level V of x is defined as the probability of observing an ε_i with at least one non-zero entry for the i^{th} input, $i = 1,...,5$, which can be written as:

$$\begin{aligned} V(x) = &\sum_{i=1}^{5} P(\varepsilon_i \neq \mathbf{0} \mid x = \text{sa0}, \text{input } i) P(x = \text{sa0}) P(\text{input } i) \\ &+ \sum_{i=1}^{5} P(\varepsilon_i \neq \mathbf{0} \mid x = \text{sa1}, \text{input } i) P(x = \text{sa1}) P(\text{input } i). \end{aligned} \tag{17}$$

Note that $\varepsilon_i \neq \mathbf{0}$ means that $\beta_i \neq \gamma_i$, i.e., normal and abnormal networks provide different output responses in the last 100 iterations for input i. Assuming equi-probable faults and equi-probable inputs [4], we have computed vulnerabilities for all individual molecules in the network using Equation (17).

Similarly, when a pair of molecules x and y is faulty, the vulnerability level V of the pair (x, y) is defined as the probability of observing an ε_i with at least one non-zero entry for the i^{th} input, $i = 1,...,5$, which can be formulated as:

$$\begin{aligned} V(x,y) = &\sum_{i=1}^{5} P(\varepsilon_i \neq \mathbf{0} \mid (x,y) = (\text{sa0},\text{sa0}), \text{input } i) P((x,y) = (\text{sa0},\text{sa0})) P(\text{input } i) \\ &+ \sum_{i=1}^{5} P(\varepsilon_i \neq \mathbf{0} \mid (x,y) = (\text{sa0},\text{sa1}), \text{input } i) P((x,y) = (\text{sa0},\text{sa1})) P(\text{input } i) \\ &+ \sum_{i=1}^{5} P(\varepsilon_i \neq \mathbf{0} \mid (x,y) = (\text{sa1},\text{sa0}), \text{input } i) P((x,y) = (\text{sa1},\text{sa0})) P(\text{input } i) \\ &+ \sum_{i=1}^{5} P(\varepsilon_i \neq \mathbf{0} \mid (x,y) = (\text{sa1},\text{sa1}), \text{input } i) P((x,y) = (\text{sa1},\text{sa1})) P(\text{input } i). \end{aligned} \tag{18}$$

Following the approach of [4], faults and inputs are considered to be equi-probable for the double-fault analysis as well. We have computed vulnerabilities for all pairs of molecules in the network using Equation (18). Note that while we assume equi-probable sa0 and sa1 faults in our computations, Equations (17) and (18) can be used for other fault probabilities, if such information is available.

C. The Hybrid LTP-Signaling Model: A Combination of the STDP-BCM Synaptic Plasticity and the Intraneuronal CREB Signaling Network

To combine the STDP-BCM synaptic plasticity model and the intraneuronal CREB signaling network model discussed in METHODS A and B, respectively, we compute $[\text{pCREB}]$ in Equation (12) as follows. The initial and steady state $[\text{pCREB}]$ values in [20] are 1 and 4, respectively. On the other hand, the initial and steady state values of $\text{CREB}_{\text{network}}$ defined and computed in METHODS B are 0 and 0.9, respectively. Given the different numerical ranges, we use the following equation to properly convert $\text{CREB}_{\text{network}}$ values to $[\text{pCREB}]$ values:

$$[\text{pCREB}] = (4-1) \times \left(\frac{\text{CREB}_{\text{network}} - 0}{0.9} \right) + 1. \tag{19}$$

CONCLUSION

In this paper, a hybrid model (Figure 1) is introduced to investigate how various signaling molecules in an intraneuronal signaling network regulating CREB (Figure 2), may affect the long term potentiation (LTP) interneuronal process. CREB, a cAMP response element-binding protein with cAMP standing for cyclic adenosine monophosphate, is a transcription factor known to be highly involved in important functions of the cognitive and executive human brain, such as learning and memory. Additionally, LTP refers to an increased synaptic strength over a long period of time among neurons, usually induced by the occurrence of an activity that generates high frequency stimulations in the brain. The hybrid LTP-signaling model is then analyzed using a proposed molecular fault diagnosis method, to quantify the importance of various signaling molecules according to how much they affect an intercellular phenomenon, when they are faulty, i.e., dysfunctional. This allows to classify and rank various intraneuronal signaling molecules based on how much their faulty behaviors affect an interneuronal process.

Fault diagnosis results of the hybrid LTP-signaling model are obtained and presented using two important synaptic plasticity parameters: *neuronal activity* and *synaptic weight*. The neuronal activity is the moving time-average of postsynaptic spike count of a neuron after receiving high frequency stimulation (HFS), whereas the synaptic weight represents the field excitatory post synaptic potential (fEPSP).

With regard to the first parameter, i.e., the neuronal activity, analysis of its variations after an HFS - when there is one faulty molecule in the intraneuronal CREB signaling network - reveals that depending on the level of impact of the faulty molecule on CREB, molecules are categorized into several classes (Figure 4). We observe that some classes of faulty molecules exhibit neuronal activities that are close to the wild-type neuronal activity, whereas others exhibit noticeable deviations from it. Given the possibility of

having more than one molecule involved in signaling failures and the development of pathological conditions, neuronal activity variations after an HFS and when there are two concurrently faulty molecules in the intraneuronal CREB signaling network are analyzed (Figure 5). We observe that depending on the level of impact of the faulty pair of molecules on CREB, pairs of molecules are categorized into many more classes, compared to the single fault scenario, and with many double fault classes being distant from the wild-type neuronal activity. Another interesting observation is that if two molecules are concurrently faulty, their damaging impact on the neuronal activity can be more profound, compared to only one of them being faulty.

For the second parameter, i.e., the synaptic weight, we observe that, in general, single and double fault behaviors are qualitatively similar to the neuronal activity parameter (Figures 7 and S4).

Possible relations between the introduced hybrid fault diagnosis and a purely intracellular fault diagnosis are studied in the paper as well. A high intracellular vulnerability for a molecule or a molecular pair means that with high probability, the whole signaling network does not respond correctly, if the molecule or the molecular pair is faulty. We observe that for the considered CREB signaling network, both the faulty neuronal activity parameter (Figure 6) and the faulty synaptic weight parameter (Figure 8) deviate more and more from their wild-type values, as the corresponding intracellular vulnerability levels increase. This can be intuitively reasonable, as one can expect that highly important intracellular faults can impair the neuronal activity and synaptic weight further.

In summary, by incorporating some interneuronal parameters and adding another dimension to the intraneuronal analysis, the introduced hybrid approach provides more information that can assist with selecting possibly more appropriate therapeutic targets. For example, in the considered hybrid system, we observe that there are several faults that exhibit the same high intracellular vulnerability level, whereas it may not be straightforward to select which one for therapeutic targeting. However, using the introduced hybrid approach, we note that in the synaptic weight additional space, those apparently similar faults become distinguished from each other, by showing different amounts of deviation from the wild-type synaptic weight. Subsequently, one may say that a fault with a high intracellular vulnerability level, while causing a large deviation from the wild-type synaptic weight is perhaps more likely to contribute to the development of the pathology and may be a better target for drug development and delivery.

ACKNOWLEDGMENTS

We are grateful to Prof. Lubica Benuskova for providing us with her original computer code.

REFERENCES

1. Sitaramayya A. Signal transduction: pathways, mechanisms and diseases. Springer 2009.
2. McConnell JL, Wadzinski BE. Targeting protein serine/threonine phosphatases for drug development. Mol. Pharmacol. 2009; **75**:1249-61.
3. Albert R, DasGupta B, Mobasheri N. Some perspectives on network modeling in therapeutic target prediction. Biomed. Eng. Comput. Biol. 2013; **5**:17-24.
4. Abdi A, Tahoori MB, Emamian ES. Fault diagnosis engineering of digital circuits can identify vulnerable molecules in complex cellular pathways. Science Signaling 2008; **1**:ra10.
5. Helikar T, Konvalina J, Heidel J, Rogers JA. Emergent decision-making in biological signal transduction networks. Proc. Natl. Acad. Sci. 2008; **105**:1913-8.
6. Saez-Rodriguez J, Alexopoulos LG, Epperlein J, et al. Discrete logic modelling as a means to link protein signalling networks with functional analysis of mammalian signal transduction. Mol. Syst. Biol. 2009; **5**:331.
7. Shmulevich I, Dougherty ER, Kim S, Zhang W. Probabilistic Boolean networks: a rule-based uncertainty model for gene regulatory networks. Bioinformatics 2002; **18**:261-74.
8. Saadatpour A, Wang RS, Liao A, et al. Dynamical and structural analysis of a T cell survival network identifies novel candidate therapeutic targets for large granular lymphocyte leukemia. PLoS Comput. Biol. 2011; **7**:e1002267.
9. Bliss TV, Lømo T. Long-lasting potentiation of synaptic transmission in the dentate area of the anaesthetized rabbit following stimulation of the perforant path. J. Physiol. 1973; **232**:331-56.
10. Nicoll RA. A brief history of long-term potentiation. Neuron 2017; **93**:281-90.
11. Bliss TV, Collingridge GL, Morris RG. Synaptic plasticity in health and disease: introduction and overview. Phil. Trans. R. Soc. B 2014; **369**:20130129.
12. Dhuriya YK, Sharma D. Neuronal plasticity: Neuronal organization is associated with neurological disorders. J. Mol. Neurosci. 2020; **70**:1684-701.
13. Nègre N, Brown CD, Ma L, et al. A cis-regulatory map of the Drosophila genome. Nature 2011; **471**:527-31.
14. Hobert O, Carrera I, Stefanakis N. The molecular and gene regulatory signature of a neuron. Trends Neurosci. 2010; **33**:435-45.
15. Pruunsild P, Sepp M, Orav E, Koppel I, Timmusk T. Identification of cis-elements and transcription factors regulating neuronal activity-dependent transcription of human BDNF gene. J. Neurosci. 2011; **31**:3295-308.
16. Rodríguez-Tornos FM, San Aniceto I, Cubelos B, Nieto M. Enrichment of conserved synaptic activity-responsive element in neuronal genes predicts a coordinated response of MEF2, CREB and SRF. PLoS One 2013; **8**:e53848.
17. Lee AP, Brenner S, Venkatesh B. Mouse transgenesis identifies conserved functional enhancers and cis-regulatory motif in the vertebrate LIM homeobox gene Lhx2 locus. PLoS One 2011; **6**:e20088.
18. Ong CT, Corces VG. Enhancer function: new insights into the regulation of tissue-specific gene expression. Nat. Rev. Genet. 2011; **12**:283-93.

19. Fontan-Lozano A, Romero-Granados R, Pérez-Villegas EM, Carrión AM. The role of CREB in neuronal plasticity, learning and memory, and in neuropsychiatric disorders. Transcription Factors CREB and NF-κB: Involvement in Synaptic Plasticity and Memory Formation 2012.

20. Benuskova L, Kasabov N. Modeling L-LTP based on changes in concentration of pCREB transcription factor. Neurocomputing 2007; **70**:2035-40.

21. Benuskova L, Rema V, Armstrong-James M, Ebner FF. Theory for normal and impaired experience-dependent plasticity in neocortex of adult rats. Proc. Natl. Acad. Sci. 2001; **98**:2797-802.

22. Bienenstock EL, Cooper LN, Munro PW. Theory for the development of neuron selectivity: orientation specificity and binocular interaction in visual cortex. J. Neurosci. 1982; **2**:32-48.

23. Habibi I, Emamian ES, Abdi A. Advanced fault diagnosis methods in molecular networks. PLoS One 2014; **9**:e108830.

24. Habibi I, Emamian ES, Abdi A. Quantitative analysis of intracellular communication and signaling errors in signaling networks. BMC Syst. Biol. 2014; **8**:1-6.

25. Izhikevich EM. Simple model of spiking neurons. IEEE Trans. Neural Netw. 2003; **14**:1569-72.

26. Benuskova L, Abraham WC. STDP rule endowed with the BCM sliding threshold accounts for hippocampal heterosynaptic plasticity. J. Comput. Neurosci. 2007; **22**:129-33.

27. Saadatpour A, Albert R. Discrete dynamic modeling of signal transduction networks. Methods Mol. Biol. 2012: 255-72.

SUPPLEMENTARY MATERIALS

5-HT1AR to Galphas[1], 5-HT1AR to Galphaz[2], 5-HT1AR to Gbetagamma[1], 5-HT2AR to Gbetagamma[3], 5-HT4R to Galphas[4], 5-HT4R to Gbetagamma[4], A1R to Galphai[5], A1R to Gbetagamma[5], A2AR to Galphas[6], A2AR to Gbetagamma[6], AC1 to cAMP[7], AC2 to cAMP[8], AC5 to cAMP[9], ACH to M1R[10], ACH to M2R[11], ACH to M4R[12], Adenosine to A1R[5], Adenosine to A2AR[13], AKT to GSK3[14], Ca^{2+} to AC5[15], Ca^{2+} to Calmodulin[16], Ca^{2+} to PKC[17], Calmodulin to AC1[18], Calmodulin to CamKII[19], Calmodulin to CamKIV[20], Calmodulin to CamKK[21], Calmodulin to mGluR7[22], Calmodulin to NMDAR[23], Calmodulin to PLCβ[24], Calmodulin to PP2B[25], CamKI to CREB[26], CamKII to CREB[26], CamKII to NtypeCaCh[27], CamKII to PP2A[28], CamKIV to CREB[29], CamKIV to CREM[30], CamKK to AKT[31], CamKK to CamKI[21], CamKK to CamKIV[32], cAMP to PKA[33], CBP to cJUN[34], cJUN to CREB[35], CREM to CREB[36], D1R to Galphai[37], D1R to Galphas[37], D1R to Gbetagamma[37], D2R to Galphai[38], D2R to Galphaz[39], D2R to Gbetagamma[40], D3R to Galphai[41], D3R to Gbetagamma[41], D3R to GRB2[42], DAG to PKC[17], Dopamine to D1R[38], Dopamine to D2R[38], Dopamine to D3R[41], Galphai to AC2[43], Galphai to AC5[43], Galphas to AC1[44], Galphas to AC2[8], Galphas to AC5[45], Galphaz to AC1[46], Galphaz to AC5[46], Gbetagamma to AC1[7], Gbetagamma to AC2[47], Gbetagamma to NtypeCaCh[48], Gbetagamma to P/QCaCh[48], Gbetagamma to PI3K[49], Gbetagamma to PLCβ[50], Gbetagamma to RASGAP[51], Glutamate to mGluR1[52], Glutamate to mGluR7[22], Glutamate to NMDAR[53], GRB2 to SAM68[54], GSK3 to cJUN[55], GSK3 to CREB[56], ILK to AKT[57], ILK to GSK3[57], M1R to Gbetagamma[58], M2R to Galphai[59], M2R to Gbetagamma[59], M4R to Galphai[12], M4R to Gbetagamma[12], mGluR1 to Gbetagamma[60], mGluR7 to Galphai[22], mGluR7 to Gbetagamma[22], NMDAR to Ca^{2+}[61], NMDAR to CamKII[23], NMDAR to PLCγ[62], NtypeCaCh to Ca^{2+}[63], P/QCaCh to Ca^{2+}[64], PDK1 to AKT[65], PDK1 to PKC[66], PDK1 to RSK[67], PI3K to PIP2[68], PI3K to PIP3[68], PIP2 to AKT[69], PIP3 to AKT[69], PIP3 to ILK[57], PIP3 to PDK1[65], PIP3 to PKC[70], PKA to CamKK[21], PKA to CBP[71], PKA to CREB[72], PKA to D1R[73], PKA to mGluR7[74], PKA to NMDAR[75], PKA to P/QCaCh[76], PKA to PLCβ[77], PKA to PLCγ[78], PKC to AC2[79], PKC to AC5[80], PKC to GSK3[81], PKC to mGluR1[82], PKC to mGluR7[22], PKC to NMDAR[83], PKC to NtypeCaCh[84], PKC to PLCβ[85], PLCβ to DAG[86], PLCβ to PIP2[87], PLCγ to DAG[88], PLCγ to PIP2[89], PP2A to AKT[90], PP2A to CamKI[91], PP2A to CamKIV[92], PP2A to CREB[93], PP2A to GSK3[14], PP2A to NMDAR[94], PP2B to CamKIV[95], PP2B to NMDAR[96], RASGAP to AKT[97], RSK to CREB[98], SAM68 to CBP[99], Serotonin to 5-HT1AR[100], Serotonin to 5-HT2AR[3], Serotonin to 5-HT4R[4]

Figure S1. Pairwise molecular interactions of the CREB intraneuronal signaling network (Figure 2). Numerical superscripts cite the references listed under Supplementary References. Note that ACH stands for acetylcholine.

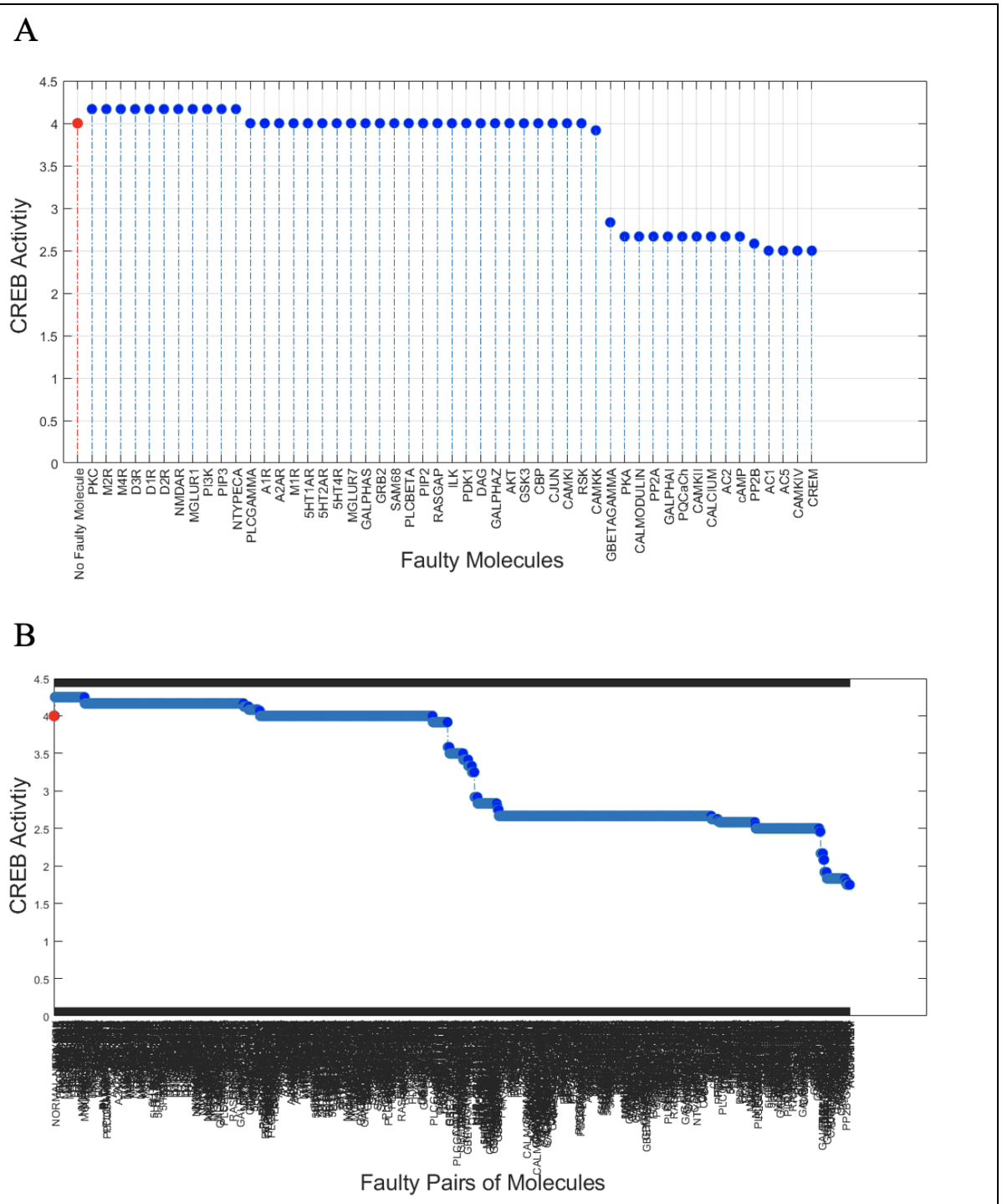

Figure S2. CREB activity level versus faulty molecules (or pair of molecules). **(A)** CREB activity level when there is one faulty molecule in the intraneuronal CREB signaling network. Depending on the faulty molecule, various activity levels are observed. **(B)** CREB activity level when there are two concurrently faulty molecules in the intraneuronal CREB signaling network. Depending on the faulty pair of molecules, various activity levels are observed. Since so many labels on the horizontal axis - representing 1275 pairs of molecules - are inevitably unreadable, a full listing of all the labels of all the pairs are provided in Table S3.1-S3.29.

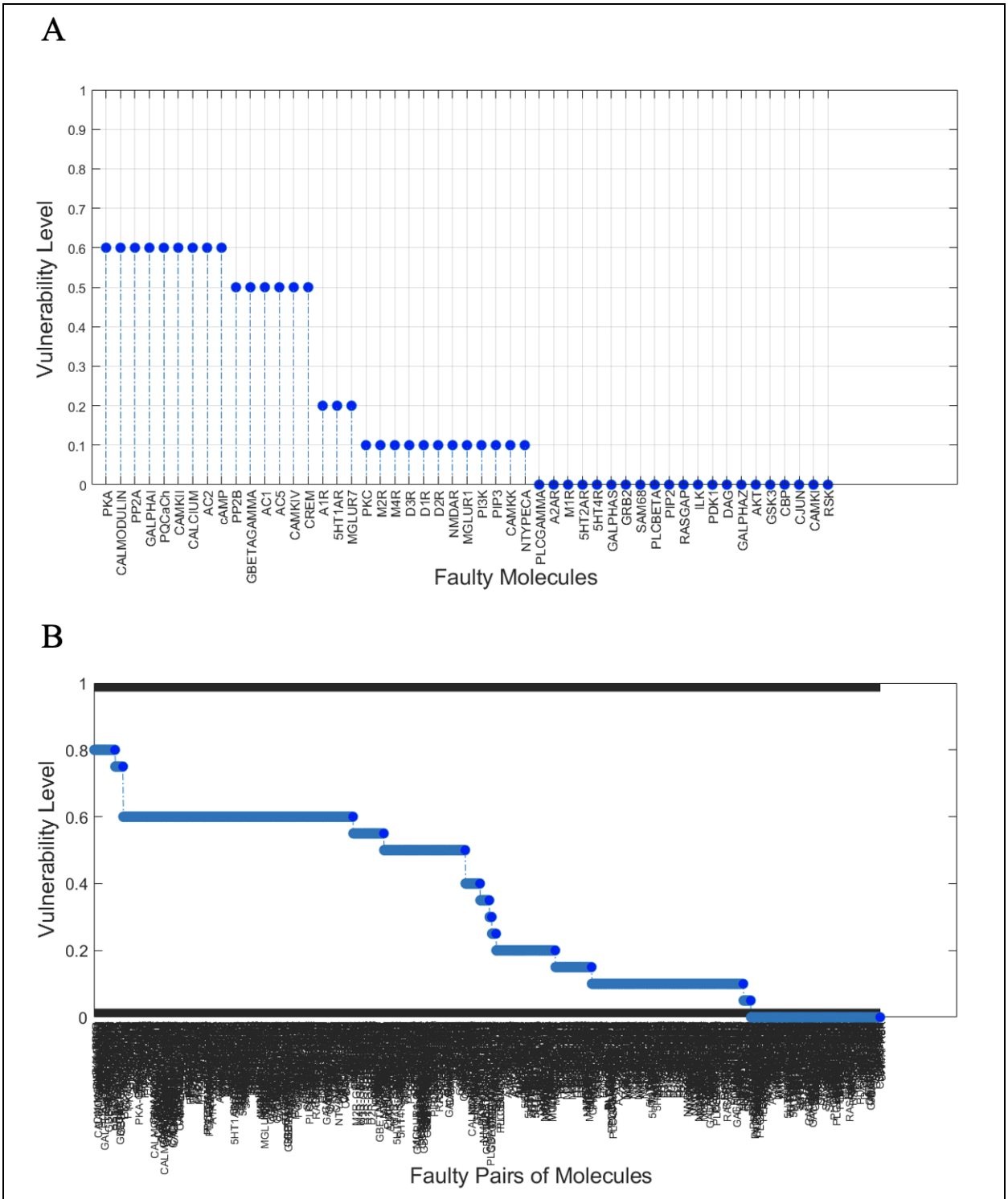

Figure S3. Vulnerability of the intraneuronal CREB signaling network to the dysfunction of one or a pair of faulty molecules. **(A)** Vulnerability of the intraneuronal CREB signaling network to the dysfunction of each of its 51 molecules. **(B)** Vulnerability of the intraneuronal CREB signaling network to the dysfunction of each of its 1275 pairs of molecules. Since such a large number of labels on the horizontal axis are inevitably unreadable, a full listing of all the labels of all the pairs and their vulnerabilities are provided in Table S5.1-S5.14.

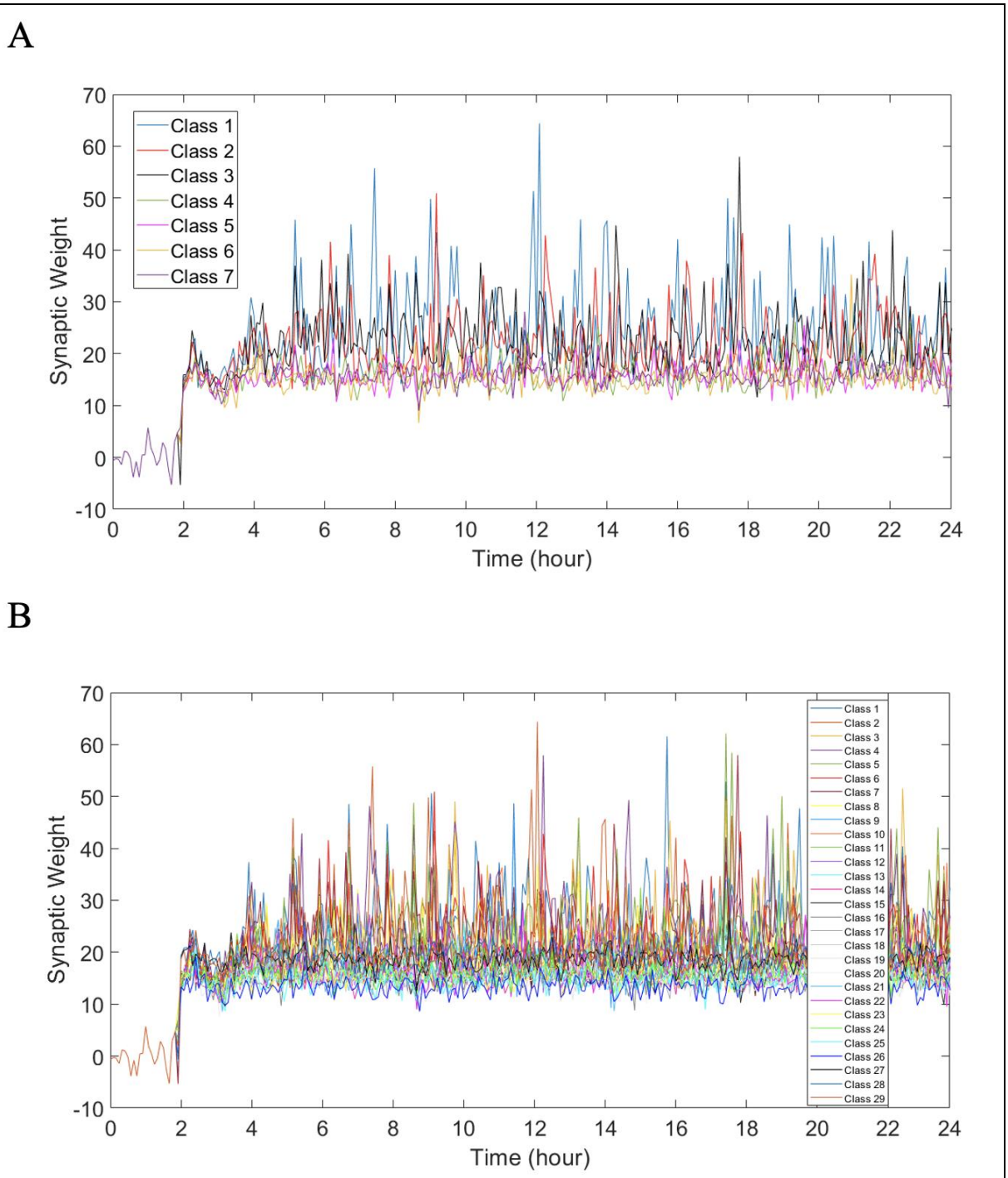

Figure S4. Synaptic weight variations versus time, when a high frequency stimulation is applied to the neuron. **(A)** Synaptic weight variations versus time, when there is one faulty molecule in the intraneuronal CREB signaling network. Depending on the level of impact of the faulty molecule on CREB, molecules are categorized to seven classes, and the corresponding synaptic weights are shown by different colors. **(B)** Synaptic weight variations versus time, when there are two concurrently faulty molecules in the intraneuronal CREB signaling network. Depending on the level of impact of the faulty pair of molecules on CREB, pairs of molecules are categorized to twenty nine classes, and the corresponding synaptic weight are shown by various colors.

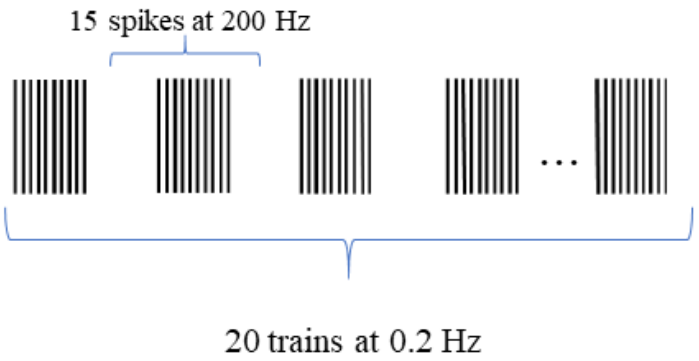

Figure S5. The high frequency stimulation protocol used to induce late long term potentiation [20].

Table S1. Regulatory equations for the CREB network molecules of Figure 2. In the equations, "x" is used for the AND operation, "+" is used for the OR operation, and "~" is used for the NOT operation. In what follows, ACH stands for acetylcholine.

Molecules	**Equations**
5-HT1AR	5-HT1AR = Serotonin
5-HT2AR	5-HT2AR = Serotonin
5-HT4R	5-HT4R = Serotonin
A1R	A1R = Adenosine
A2AR	A2AR = Adenosine
AC1	AC1 = ~Galphaz x ~Gbetagamma x (Calmodulin + Galphas)
AC2	AC2 = ~Galphai x (Galphas + Gbetagamma + PKC)
AC5	AC5 = ~Galphai x ~Galphaz x ~Ca^{2+} x (Galphas + PKC)
AKT	AKT = ~PP2A x (CamKK + PIP2 + PIP3 + PDK1 + ILK + RASGAP)
Ca^{2+}	Ca^{2+} = NMDAR + P/QCaCh + NtypeCaCh
Calmodulin	Calmodulin = Ca^{2+}
CamKI	CamKI = ~PP2A x CamKK
CamKII	CamKII = Calmodulin + NMDAR
CamKIV	CamKIV = ~PP2A x ~PP2B x (Calmodulin + CamKK)
CamKK	CamKK = ~PKA x Calmodulin
cAMP	cAMP = AC1 + AC2 + AC5
CBP	CBP = ~SAM68 x PKA
cJUN	cJUN = ~GSK3 x CBP
CREB	CREB = ~CREM x ~PP2A x (CamKI + CamKII + CamKIV + RSK + PKA + GSK3 + cJUN)
CREM	CREM = CamKIV
D1R	D1R = ~PKA x Dopamine
D2R	D2R = Dopamine
D3R	D3R = Dopamine
DAG	DAG = PLCγ + PLCβ
Galphai	Galphai = A1R + D1R + D2R + D3R + 5-HT1AR + M2R + M4R + mGluR7

Molecules	**Equations**
Galphas	Galphas = A2AR + D1R + 5-HT1AR + 5-HT4R
Galphaz	Galphaz = D2R + 5-HT1AR
Gbetagamma	Gbetagamma = $mGluR_1$ + $mGluR_7$ + M1R + M2R + M4R + 5-HT1AR + 5-HT2AR + 5-HT4R + D1R + D2R + D3R + A1R + A2AR
GRB2	GRB2 = D3R
GSK3	GSK3 = ~ILK x ~AKT x ~PKC x PP2A
ILK	ILK = PIP3
M1R	M1R = ACH
M2R	M2R = ACH
M4R	M4R = ACH
$mGluR_1$	$mGluR_1$ = PKC + Glutamate
$mGluR_7$	$mGluR_7$ = ~Calmodulin x (PKC + PKA + Glutamate)
NMDAR	NMDAR = ~PKC x ~PP2A x ~Calmodulin x ~PP2B x (PKA + Glutamate)
NtypeCaCh	NtypeCaCh = ~Gbetagamma x (PKC + CamKII)
P/QCaCh	P/QCaCh = ~PKA x Gbetagamma
PDK1	PDK1 = PIP3
PI3K	PI3K = Gbetagamma
PIP2	PIP2 = ~PLCγ x ~PLCβ x ~PI3K
PIP3	PIP3 = PI3K
PKA	PKA = cAMP
PKC	PKC = PIP3 + PDK1 + DAG + Ca^{2+}
PLCβ	PLCβ = ~PKA x ~PKC x (Calmodulin + Gbetagamma)
PLCγ	PLCγ = ~PKA x NMDAR
PP2A	PP2A = ~CamKII
PP2B	PP2B = Calmodulin
RASGAP	RASGAP = Gbetagamma
RSK	RSK = PDK1
SAM68	SAM68 = GRB2

Table S2. CREB activity level when there is one faulty molecule in the intraneuronal CREB signaling network. Depending on the level of impact of the faulty molecule on CREB, molecules are categorized to seven classes.

CREB Activity Level	Class No.	Faulty Molecules
4.167	1	PKC/ M2R/ M4R/ D3R/ D1R/ D2R/ NMDAR/ MGLUR1/ PI3K/ PIP3/ NTYPECA
4	2	PLCGAMMA/ A1R/ A2AR/ M1R/ 5HT1AR/ 5HT2AR/ 5HT4R/ MGLUR7/ GALPHAS/ GRB2/ SAM68/ PLCBETA/ PIP2/ RASGAP/ ILK/ PDK1/ DAG/ GALPHAZ/ AKT/ GSK3/ CBP/ CJUN/ CAMKI/ RSK
3.917	3	CAMKK
2.833	4	GBETAGAMMA
2.667	5	PKA/ CALMODULIN/ PP2A/ GALPHAI/ PQCaCh/ CAMKII/ CALCIUM/ AC2/ cAMP
2.583	6	PP2B
2.5	7	AC1/ AC5/ CAMKIV/ CREM

Table S3.1. CREB activity level with two concurrently faulty molecules in the signaling network. Depending on the level of impact of the faulty pair of molecules on CREB, pairs of molecules are categorized to twenty nine classes.

CREB Activity Level	**Faulty Pairs of Molecules (Class 1)**	
4.25	PKC-M2R/ PKC-M4R	D3R-D1R/ D3R-D2R
	PKC-D3R/ PKC-D1R	D3R-NMDAR/ D3R-MGLUR1
	PKC-D2R/ PKC-MGLUR1	D3R-PI3K/ D3R-PIP3
	PKC-NTYPECA/ M2R-D3R	D3R-NTYPECA/ D1R-D2R
	M2R-D1R/ M2R-D2R	D1R-NMDAR/ D1R-MGLUR1
	M2R-NMDAR/ M2R-MGLUR1	D1R-PI3K/ D1R-PIP3
	M2R-PI3K/ M2R-PIP3	D1R-NTYPECA/ D2R-NMDAR
	M2R-NTYPECA/ M4R-D3R	D2R-MGLUR1/ D2R-PI3K
	M4R-D1R/ M4R-D2R	D2R-PIP3/ D2R-NTYPECA
	M4R-NMDAR/ M4R-MGLUR1	NMDAR-MGLUR1/ NMDAR-NTYPECA
	PIP3-NTYPECA/ M4R-PI3K	MGLUR1-PI3K/ MGLUR1-PIP3
	M4R-PIP3/ M4R-NTYPECA	MGLUR1-NTYPECA/ PI3K-NTYPECA

Table S3.2. CREB activity level with two concurrently faulty molecules in the signaling network.

CREB Activity Level	Faulty Pairs of Molecules (Class 2)			
4.167	PKC-PLCGAMMA	A2AR-NMDAR	NMDAR-MGLUR7	D1R-PDK1
	PKC-A1R	A2AR-PI3K	NMDAR-GALPHAS	D1R-DAG
	PKC-A2AR	A2AR-PIP3	NMDAR-GRB2	D1R-GALPHAZ
	PKC-M1R	A2AR-NTYPECA	NMDAR-SAM68	D1R-AKT
	PKC-5HT1AR	M1R-M2R	NMDAR-PLCBETA	D1R-GSK3
	PKC-5HT2AR	M1R-M4R	NMDAR-PI3K	D1R-CBP
	PKC-5HT4R	M1R-D3R	NMDAR-PIP2	D1R-CJUN
	PKC-NMDAR	M1R-D1R	NMDAR-RASGAP	D1R-CAMKI
	PKC-MGLUR7	M1R-D2R	NMDAR-PIP3	D1R-RSK
	PKC-GALPHAS	M1R-NMDAR	NMDAR-ILK	D2R-MGLUR7
	PKC-GRB2	M1R-PI3K	NMDAR-PDK1	D2R-GALPHAS
	PKC-SAM68	M1R-PIP3	NMDAR-DAG	D2R-GRB2
	PKC-PLCBETA	M1R-NTYPECA	NMDAR-GALPHAZ	D2R-SAM68
	PKC-PI3K	M2R-M4R	NMDAR-AKT	D2R-PLCBETA
	PKC-PIP2	M2R-5HT1AR	NMDAR-GSK3	D2R-PIP2
	PKC-RASGAP	M2R-5HT2AR	NMDAR-CBP	D2R-RASGAP
	PKC-PIP3	M2R-5HT4R	NMDAR-CJUN	D2R-ILK
	PKC-ILK	M2R-MGLUR7	NMDAR-CAMKI	D2R-PDK1
	PKC-PDK1	M2R-GALPHAS	NMDAR-RSK	D2R-DAG
	PKC-DAG	M2R-GRB2	MGLUR1-MGLUR7	D2R-GALPHAZ
	PKC-GALPHAZ	M2R-SAM68	MGLUR1-GALPHAS	D2R-AKT
	PKC-AKT	M2R-PLCBETA	MGLUR1-GRB2	D2R-GSK3
	PKC-GSK3	M2R-PIP2	MGLUR1-SAM68	D2R-CBP
	PKC-CBP	M2R-RASGAP	MGLUR1-PLCBETA	D2R-CJUN
	PKC-CJUN	M2R-ILK	MGLUR1-PIP2	D2R-CAMKI
	PKC-CAMKI	M2R-PDK1	MGLUR1-ILK	D2R-RSK
	PKC-RSK	M2R-DAG	MGLUR1-RASGAP	5HT1AR-PI3K
	PLCGAMMA-M2R	M2R-GALPHAZ	MGLUR1-PDK1	5HT1AR-PIP3

4.167	PLCGAMMA-M4R PLCGAMMA-D3R PLCGAMMA-D1R PLCGAMMA-D2R PLCGAMMA-NMDAR PLCGAMMA-MGLUR1 PLCGAMMA-NTYPECA A1R-M2R A1R-M4R A1R-D3R A1R-D1R A1R-D2R A1R-NMDAR A1R-PI3K A1R-PIP3 A1R-NTYPECA A2AR-M2R A2AR-M4R A2AR-D3R A2AR-D1R A2AR-D2R D3R-RSK D1R-MGLUR7 D1R-GALPHAS D1R-GRB2 D1R-SAM68 D1R-PLCBETA D1R-PIP2 D1R-RASGAP	M2R-AKT M2R-GSK3 M2R-CBP M2R-CJUN M2R-CAMKI M2R-RSK M4R-5HT1AR M4R-5HT2AR M4R-5HT4R M4R-MGLUR7 M4R-GALPHAS M4R-GRB2 M4R-SAM68 M4R-PLCBETA M4R-PIP2 M4R-RASGAP M4R-ILK M4R-PDK1 M4R-DAG M4R-GALPHAZ M4R-AKT M4R-GSK3 M4R-CBP M4R-CJUN M4R-CAMKI M4R-RSK 5HT1AR-D3R 5HT1AR-D1R 5HT1AR-D2R	MGLUR1-DAG MGLUR1-GALPHAZ MGLUR1-AKT MGLUR1-GSK3 MGLUR1-CBP MGLUR1-CJUN MGLUR1-CAMKI MGLUR1-RSK MGLUR7-NTYPECA GALPHAS-PI3K GALPHAS-PIP3 GALPHAS-NTYPECA GRB2-PI3K GRB2-PIP3 GRB2-NTYPECA SAM68-PI3K SAM68-PIP3 SAM68-NTYPECA PLCBETA-NTYPECA PI3K-PIP2 PI3K-RASGAP PI3K-PIP3 PI3K-ILK PI3K-GALPHAZ PI3K-AKT PI3K-GSK3 PI3K-CBP PI3K-CJUN PI3K-CAMKI	5HT1AR-NTYPECA 5HT2AR-D3R 5HT2AR-D1R 5HT2AR-D2R 5HT2AR-NMDAR 5HT2AR-PI3K 5HT2AR-PIP3 5HT2AR-NTYPECA 5HT4R-D3R 5HT4R-D1R 5HT4R-D2R 5HT4R-NMDAR 5HT4R-PI3K 5HT4R-PIP3 5HT4R-NTYPECA D3R-MGLUR7 D3R-GALPHAS D3R-GRB2 D3R-SAM68 D3R-PLCBETA D3R-PIP2 D3R-RASGAP D3R-ILK D3R-PDK1 D3R-DAG D3R-GALPHAZ D3R-AKT D3R-GSK3 D3R-CBP

Table S3.3. CREB activity level with two concurrently faulty molecules in the signaling network.

CREB Activity Level	Faulty Pairs of Molecules (Class 3)
4.125	M2R-CAMK/ M4R-CAMKK/ D3R-CAMKK/ D1R-CAMKK D2R-CAMKK/ NMDAR-CAMKK/ MGLUR1-CAMKK/ CAMKK-NTYPECA

Table S3.4. CREB activity level with two concurrently faulty molecules in the signaling network.

CREB Activity Level	Faulty Pairs of Molecules (Class 4)
4.085	PLCGAMMA-PI3K/ PLCGAMMA-PIP3/ A1R-5HT1AR/ A1R-MGLUR1 A2AR-MGLUR1/ M1R-MGLUR1/ 5HT1AR-MGLUR1/ 5HT2AR-MGLUR1 5HT4R-MGLUR1/ PLCBETA-PI3K/ PLCBETA-PIP3 PI3K-PDK1/ PI3K-DAG/ PIP3-PDK1/ PIP3-DAG

Table S3.5. CREB activity level with two concurrently faulty molecules in the signaling network.

CREB Activity Level	Faulty Pairs of Molecules (Class 5)
4.068	PKC-CAMKK/ PI3K-CAMKK/ PIP3-CAMKK

Table S3.6. CREB activity level with two concurrently faulty molecules in the signaling network.

CREB Activity Level	Faulty Pairs of Molecules (Class 6)			
4	PLCGAMMA-A1R	M1R-GRB2	MGLUR7-RSK	RASGAP-GALPHAZ
	PLCGAMMA-A2AR	M1R-SAM68	GALPHAS-GRB2	RASGAP-AKT
	PLCGAMMA-M1R	M1R-PLCBETA	GALPHAS-SAM68	RASGAP-GSK3
	PLCGAMMA-5HT1AR	M1R-PIP2	GALPHAS-PLCBETA	RASGAP-CBP
	PLCGAMMA-5HT2AR	M1R-RASGAP	GALPHAS-PIP2	RASGAP-CJUN
	PLCGAMMA-5HT4R	M1R-ILK	GALPHAS-RASGAP	RASGAP-CAMKI
	PLCGAMMA-MGLUR7	M1R-PDK1	GALPHAS-ILK	RASGAP-RSK
	PLCGAMMA-GALPHAS	M1R-DAG	GALPHAS-PDK1	ILK-PDK1
	PLCGAMMA-GRB2	M1R-GALPHAZ	GALPHAS-DAG	ILK-DAG
	PLCGAMMA-SAM68	M1R-AKT	GALPHAS-GALPHAZ	ILK-GALPHAZ
	PLCGAMMA-PLCBETA	M1R-GSK3	GALPHAS-AKT	ILK-AKT
	PLCGAMMA-PIP2	M1R-CBP	GALPHAS-GSK3	ILK-GSK3
	PLCGAMMA-RASGAP	M1R-CJUN	GALPHAS-CBP	ILK-CBP
	PLCGAMMA-ILK	M1R-CAMKI	GALPHAS-CJUN	ILK-CJUN
	PLCGAMMA-PDK1	M1R-RSK	GALPHAS-CAMKI	ILK-CAMKI
	PLCGAMMA-DAG	5HT1AR-5HT2AR	GALPHAS-RSK	ILK-RSK
	PLCGAMMA-GALPHAZ	5HT1AR-5HT4R	GRB2-SAM68	PDK1-DAG
	PLCGAMMA-AKT	5HT1AR-MGLUR7	GRB2-PLCBETA	PDK1-GALPHAZ
	PLCGAMMA-GSK3	5HT1AR-GALPHAS	GRB2-PIP2	PDK1-AKT
	PLCGAMMA-CBP	5HT1AR-GRB2	GRB2-RASGAP	PDK1-GSK3
	PLCGAMMA-CJUN	5HT1AR-SAM68	GRB2-ILK	PDK1-CBP
	PLCGAMMA-CAMKI	5HT1AR-PLCBETA	GRB2-PDK1	PDK1-CJUN
	PLCGAMMA-RSK	5HT1AR-PIP2	GRB2-DAG	PDK1-CAMKI
	A1R-M1R	5HT1AR-RASGAP	GRB2-GALPHAZ	PDK1-RSK
	A1R-5HT2AR	5HT1AR-ILK	GRB2-AKT	DAG-GALPHAZ
	A1R-5HT4R	5HT1AR-PDK1	GRB2-GSK3	DAG-AKT
	A1R-MGLUR7	5HT1AR-DAG	GRB2-CBP	DAG-GSK3
	A1R-GALPHAS	5HT2AR-GALPHAZ	GRB2-CJUN	DAG-CBP
	A1R-GRB2	5HT2AR-AKT	GRB2-CAMKI	

	A1R-SAM68	5HT2AR-GSK3	GRB2-RSK	DAG-CJUN
	A1R-PLCBETA	5HT2AR-CBP	SAM68-PLCBETA	DAG-CAMKI
	A1R-PIP2	5HT2AR-CJUN	SAM68-PIP2	DAG-RSK
	A1R-RASGAP	5HT2AR-CAMKI	SAM68-RASGAP	GALPHAZ-AKT
	A1R-ILK	5HT2AR-RSK	SAM68-ILK	GALPHAZ-GSK3
	A1R-PDK1	5HT4R-MGLUR7	SAM68-PDK1	GALPHAZ-CBP
	A1R-DAG	5HT4R-GALPHAS	SAM68-DAG	GALPHAZ-CJUN
	A1R-GALPHAZ	5HT4R-GRB2	SAM68-GALPHAZ	GALPHAZ-CAMKI
	A1R-AKT	5HT4R-SAM68	SAM68-AKT	GALPHAZ-RSK
	A1R-GSK3	5HT4R-PLCBETA	SAM68-GSK3	AKT-GSK3
	A1R-CBP	5HT4R-PIP2	SAM68-CBP	AKT-CBP
	A1R-CJUN	5HT4R-RASGAP	SAM68-CJUN	AKT-CJUN
	A1R-CAMKI	5HT4R-ILK	SAM68-CAMKI	AKT-CAMKI
	A1R-RSK	5HT4R-PDK1	SAM68-RSK	AKT-RSK
4	A2AR-M1R	5HT4R-DAG	PLCBETA-PIP2	GSK3-CBP
	A2AR-5HT1AR	5HT4R-GALPHAZ	PLCBETA-RASGAP	GSK3-CJUN
	A2AR-5HT2AR	5HT4R-AKT	PLCBETA-ILK	GSK3-CAMKI
	A2AR-5HT4R	5HT4R-GSK3	PLCBETA-PDK1	GSK3-RSK
	A2AR-MGLUR7	5HT4R-CBP	PLCBETA-DAG	CBP-CJUN
	A2AR-GALPHAS	5HT4R-CJUN	PLCBETA-GALPHAZ	CBP-CAMKI
	A2AR-GRB2	5HT4R-CAMKI	PLCBETA-AKT	CBP-RSK
	A2AR-SAM68	5HT4R-RSK	PLCBETA-GSK3	CJUN-CAMKI
	A2AR-PLCBETA	MGLUR7-GALPHAS	PLCBETA-CBP	CJUN-RSK
	A2AR-PIP2	MGLUR7-GRB2	PLCBETA-CJUN	CAMKI-RSK
	A2AR-RASGAP	MGLUR7-SAM68	PLCBETA-CAMKI	
	A2AR-ILK	MGLUR7-PLCBETA	PLCBETA-RSK	
	A2AR-PDK1	MGLUR7-PI3K	PIP2-RASGAP	
	A2AR-DAG	MGLUR7-PIP2	PIP2-ILK	
	A2AR-GALPHAZ	MGLUR7-RASGAP	PIP2-PDK1	
	A2AR-AKT	MGLUR7-PIP3	PIP2-DAG	
	A2AR-GSK3	MGLUR7-ILK	PIP2-GALPHAZ	
	A2AR-CBP	MGLUR7-PDK1	PIP2-AKT	

4	A2AR-CJUN A2AR-CAMKI A2AR-RSK M1R-5HT1AR M1R-5HT2AR M1R-5HT4R M1R-MGLUR7 M1R-GALPHAS	MGLUR7-DAG MGLUR7-GALPHAZ MGLUR7-CAMKK MGLUR7-AKT MGLUR7-GSK3 MGLUR7-CBP MGLUR7-CJUN MGLUR7-CAMKI	PIP2-GSK3 PIP2-CBP PIP2-CJUN PIP2-CAMKI PIP2-RSK RASGAP-ILK RASGAP-PDK1 RASGAP-DAG	

Table S3.7. CREB activity level with two concurrently faulty molecules in the signaling network.

CREB Activity Level	**Faulty Pairs of Molecules (Class 7)**
3.917	PLCGAMMA-CAMKK/ A1R-A2AR/ A1R-CAMKK/ A2AR-CAMKK/ M1R-CAMKK 5HT1AR-CAMKK/ 5HT2AR-CAMKK/ 5HT4R-CAMKK/ GALPHAS-CAMKK GRB2-CAMKK/ SAM68-CAMKK/ PLCBETA-CAMKK/ PIP2-CAMKK/ RASGAP-CAMKK ILK-CAMKK/ PDK1-CAMKK/ DAG-CAMKK/ GALPHAZ-CAMKK/ CAMKK-AKT CAMKK-GSK3/ CAMKK-CBP/ CAMKK-CJUN/ CAMKK-CAMKI/ CAMKK-RSK

Table S3.8. CREB activity level with two concurrently faulty molecules in the signaling network.

CREB Activity Level	**Faulty Pairs of Molecules (Class 8)**
3.583	PKC-GBETAGAMMA/ GBETAGAMMA-PI3K/ GBETAGAMMA-PIP3

Table S3.9. CREB activity level with two concurrently faulty molecules in the signaling network.

CREB Activity Level	Faulty Pairs of Molecules (Class 9)
3.5	PKC-PKA/ PKC-GALPHAI/ PKC-AC2/ PKC-cAMP/ PKA-NMDAR PKA-PI3K/ PKA-PIP3/ PKA-NTYPECA/ CALMODULIN-NMDAR PLCGAMMA-GBETAGAMMA/ NMDAR-GALPHAI/ NMDAR-PQCaCh NMDAR-CALCIUM/ NMDAR-AC2/ NMDAR-cAMP/ GALPHAI-NTYPECA GBETAGAMMA-PLCBETA/ GBETAGAMMA-PDK1/ GBETAGAMMA-DAG PQCaCh-NTYPECA/ NTYPECA-AC2/ NTYPECA-cAMP

Table S3.10. CREB activity level with two concurrently faulty molecules in the signaling network.

CREB Activity Level	Faulty Pairs of Molecules (Class 10)
3.417	PKC-AC1/ PKC-AC5/ NMDAR-GBETAGAMMA NMDAR-AC1/ NMDAR-AC5/ GBETAGAMMA-NTYPECA NTYPECA-AC1/ NTYPECA-AC5

Table S3.11. CREB activity level with two concurrently faulty molecules in the signaling network.

CREB Activity Level	Faulty Pairs of Molecules (Class 11)
3.333	GALPHAI-PI3K/ GALPHAI-PIP3/ PI3K-AC2 PI3K-cAMP/ PIP3-AC2/ PIP3-cAMP

Table S3.12. CREB activity level with two concurrently faulty molecules in the signaling network.

CREB Activity Level	Faulty Pairs of Molecules (Class 12)
3.25	PI3K-AC1/ PI3K-AC5/ PIP3-AC1/ PIP3-AC5

Table S3.13. CREB activity level with two concurrently faulty molecules in the signaling network.

CREB Activity Level	Faulty Pairs of Molecules (Class 13)
2.917	M2R-GBETAGAMMA/ M4R-GBETAGAMMA/ D3R-GBETAGAMMA D1R-GBETAGAMMA/ D2R-GBETAGAMMA

Table S3.14. CREB activity level with two concurrently faulty molecules in the signaling network.

CREB Activity Level	Faulty Pairs of Molecules (Class 14)		
2.833	PKC-CALMODULIN PKC-PQCaCh PKC-CALCIUM PKA-MGLUR1 PKA-GBETAGAMMA A1R-GBETAGAMMA A2AR-GBETAGAMMA M1R-GBETAGAMMA 5HT1AR-GBETAGAMMA 5HT2AR-GBETAGAMMA 5HT4R-GBETAGAMMA	MGLUR1-GALPHAI MGLUR1-GBETAGAMMA MGLUR1-PQCaCh MGLUR1-AC2 MGLUR1-cAMP MGLUR7-GBETAGAMMA GALPHAS-GBETAGAMMA GBETAGAMMA-PQCaCh GBETAGAMMA-GRB2 GBETAGAMMA-SAM68 GBETAGAMMA-PIP2	GBETAGAMMA-RASGAP GBETAGAMMA-ILK GBETAGAMMA-GALPHAZ GBETAGAMMA-AKT GBETAGAMMA-GSK3 GBETAGAMMA-CBP GBETAGAMMA-CJUN GBETAGAMMA-CAMKI GBETAGAMMA-RSK

Table S3.15. CREB activity level with two concurrently faulty molecules in the signaling network.

CREB Activity Level	**Faulty Pairs of Molecules (Class 15)**
2.792	GBETAGAMMA-CAMKK

Table S3.16. CREB activity level with two concurrently faulty molecules in the signaling network.

CREB Activity Level	**Faulty Pairs of Molecules (Class 16)**
2.75	MGLUR1-AC1/ MGLUR1-AC5

Table S3.17. CREB activity level with two concurrently faulty molecules in the signaling network.

CREB Activity Level	Faulty Pairs of Molecules (Class 17)		
2.67	PKC-PP2A	CALMODULIN-GALPHAZ	M1R-GALPHAI
	PKC-CAMKII		M1R-PQCaCh
	PKA-CALMODULIN	CALMODULIN-CAMKII	M1R-CAMKII
	PKA-PP2A		M1R-CALCIUM
	PKA-PLCGAMMA	CALMODULIN-CAMKK	M1R-AC2
	PKA-A1R		M1R-cAMP
	PKA-A2AR	CALMODULIN-NTYPECA	M2R-GALPHAI
	PKA-M1R		M2R-PQCaCh
	PKA-M2R	CALMODULIN-AKT	M2R-CAMKII
	PKA-M4R	CALMODULIN-CALCIUM	M2R-CALCIUM
	PKA-5HT1AR		M2R-AC2
	PKA-5HT2AR	CALMODULIN-AC1	M2R-cAMP
	PKA-5HT4R	CALMODULIN-AC5	M4R-GALPHAI
	PKA-D3R	CALMODULIN-AC2	M4R-PQCaCh
	PKA-D1R	CALMODULIN-cAMP	M4R-CAMKII
	PKA-D2R	CALMODULIN-GSK3	M4R-CALCIUM
	PKA-MGLUR7	CALMODULIN-CBP	M4R-AC2
	PKA-GALPHAI	CALMODULIN-CJUN	M4R-cAMP
	PKA-GALPHAS	CALMODULIN-CAMKI	5HT1AR-GALPHAI
	PKA-PQCaCh		5HT1AR-PQCaCh
	PKA-GRB2	CALMODULIN-RSK	5HT1AR-CAMKII
	PKA-SAM68	PP2A-PLCGAMMA	5HT1AR-CALCIUM
	PKA-PLCBETA	PP2A-A1R	5HT1AR-AC2
	PKA-PIP2	PP2A-A2AR	5HT1AR-cAMP
	PKA-RASGAP	PP2A-M1R	5HT2AR-GALPHAI
	PKA-ILK	PP2A-M2R	5HT2AR-PQCaCh
	PKA-PDK1	PP2A-M4R	5HT2AR-CAMKII

	PKA-DAG	PP2A-5HT1AR	5HT2AR-CALCIUM
	PKA-GALPHAZ	PP2A-5HT2AR	5HT2AR-AC2
	PKA-CAMKII	PP2A-5HT4R	5HT2AR-cAMP
	PKA-CAMKK	PP2A-D3R	5HT4R-GALPHAI
	PKA-AKT	PP2A-D1R	5HT4R-PQCaCh
	PKA-CALCIUM	PP2A-D2R	5HT4R-CAMKII
	PKA-AC1	PP2A-NMDAR	5HT4R-CALCIUM
	PKA-AC5	PP2A-MGLUR1	5HT4R-AC2
	PKA-AC2	PP2A-MGLUR7	5HT4R-cAMP
	PKA-cAMP	PP2A-GALPHAI	D3R-GALPHAI
	PKA-GSK3	PP2A-GALPHAS	D3R-PQCaCh
2.67	PKA-CBP	PP2A-PQCaCh	D3R-CAMKII
	PKA-CJUN	PP2A-GRB2	D3R-CALCIUM
	PKA-CAMKI	PP2A-SAM68	D3R-AC2
	PKA-RSK	PP2A-PLCBETA	D3R-cAMP
	CALMODULIN-PP2A	PP2A-PI3K	D1R-GALPHAI
	CALMODULIN-PLCGAMMA	PP2A-PIP2	D1R-PQCaCh
	CALMODULIN-A1R	PP2A-RASGAP	D1R-CAMKII
	CALMODULIN-A2AR	PP2A-PIP3	D1R-CALCIUM
	CALMODULIN-M1R	PP2A-ILK	D1R-AC2
	CALMODULIN-M2R	PP2A-DAG	D1R-cAMP
	CALMODULIN-M4R	PP2A-GALPHAZ	D2R-GALPHAI
	CALMODULIN-5HT1AR	PP2A-CAMKII	D2R-PQCaCh
	CALMODULIN-5HT2AR	PP2A-NTYPECA	D2R-CAMKII
	CALMODULIN-5HT4R	PP2A-AKT	D2R-CALCIUM
	CALMODULIN-D3R	PP2A-CALCIUM	D2R-AC2
	CALMODULIN-D1R	PP2A-AC1	D2R-cAMP
	CALMODULIN-D2R	PP2A-AC5	NMDAR-CAMKII
	CALMODULIN-MGLUR1	PP2A-AC2	MGLUR1-CAMKII
	CALMODULIN-MGLUR7	PP2A-cAMP	MGLUR1-CALCIUM
	CALMODULIN-GALPHAI	PP2A-GSK3	MGLUR7-GALPHAI
	CALMODULIN-GALPHAS	PP2A-CBP	MGLUR7-PQCaCh

2.67	CALMODULIN-GBETAGAMMA	PP2A-CJUN	MGLUR7-CAMKII
	CALMODULIN-PQCaCh	PP2A-CAMKI	MGLUR7-CALCIUM
	CALMODULIN-GRB2	PLCGAMMA-GALPHAI	MGLUR7-AC2
	CALMODULIN-SAM68	PLCGAMMA-PQCaCh	MGLUR7-cAMP
	CALMODULIN-PLCBETA	PLCGAMMA-CAMKII	GALPHAI-GALPHAS
	CALMODULIN-PI3K	PLCGAMMA-CALCIUM	GALPHAI-PQCaCh
	CALMODULIN-PIP2	PLCGAMMA-AC2	GALPHAI-GRB2
	CALMODULIN-RASGAP	PLCGAMMA-cAMP	GALPHAI-SAM68
	CALMODULIN-PIP3	A1R-GALPHAI	GALPHAI-PLCBETA
	CALMODULIN-ILK	A1R-PQCaCh	GALPHAI-PIP2
	CALMODULIN-PDK1	A1R-CAMKII	GALPHAI-RASGAP
	CALMODULIN-DAG	A1R-CALCIUM	GALPHAI-ILK
	GALPHAI-GALPHAZ	A1R-AC2	GALPHAI-PDK1
	GALPHAI-CAMKII	A1R-cAMP	GALPHAI-DAG
	GALPHAI-CAMKK	A2AR-GALPHAI	PQCaCh-DAG
	GALPHAI-AKT	A2AR-PQCaCh	PQCaCh-CAMKII
	GALPHAI-CALCIUM	A2AR-CAMKII	PQCaCh-CAMKK
	GALPHAI-AC2	A2AR-CALCIUM	PQCaCh-AKT
	GALPHAI-cAMP	A2AR-AC2	PQCaCh-CALCIUM
	GALPHAI-GSK3	A2AR-cAMP	PQCaCh-AC1
	GALPHAI-CBP	PQCaCh-GRB2	PQCaCh-AC5
	GALPHAI-CJUN	PQCaCh-SAM68	PQCaCh-AC2
	GALPHAI-CAMKI	PQCaCh-PLCBETA	PQCaCh-cAMP
	GALPHAI-RSK	PQCaCh-PI3K	PQCaCh-GALPHAZ
	GALPHAS-PQCaCh	PQCaCh-PIP2	PQCaCh-GSK3
	GALPHAS-CAMKII	PQCaCh-RASGAP	PQCaCh-CBP
	GALPHAS-CALCIUM	PQCaCh-PIP3	PQCaCh-CJUN
	GALPHAS-AC2	PQCaCh-ILK	PQCaCh-CAMKI
	GALPHAS-cAMP	PQCaCh-PDK1	PQCaCh-RSK
	GBETAGAMMA-CAMKII		GRB2-CAMKII
	GBETAGAMMA-CALCIUM		GRB2-CALCIUM

	GRB2-AC2	DAG-AC2	CALCIUM-CAMKI
	GRB2-cAMP	DAG-cAMP	CALCIUM-RSK
	SAM68-CAMKII	GALPHAZ-CAMKII	AC1-cAMP
	SAM68-CALCIUM	GALPHAZ-CALCIUM	AC5-cAMP
	SAM68-AC2	GALPHAZ-AC2	AC2-cAMP
	SAM68-cAMP	GALPHAZ-cAMP	AC2-GSK3
	PLCBETA-CAMKII	CAMKII-NTYPECA	AC2-CBP
	PLCBETA-CALCIUM	CAMKII-AKT	AC2-CJUN
	PLCBETA-AC2	CAMKII-CALCIUM	AC2-CAMKI
	PLCBETA-cAMP	CAMKII-AC1	AC2-RSK
	PI3K-CAMKII	CAMKII-AC5	cAMP-GSK3
	PI3K-CALCIUM	CAMKII-AC2	cAMP-CBP
	PIP2-CAMKII	CAMKII-cAMP	cAMP-CJUN
	PIP2-CALCIUM	CAMKII-GSK3	cAMP-CAMKI
	PIP2-AC2	CAMKII-CBP	cAMP-RSK
	PIP2-cAMP	CAMKII-CJUN	
2.67	RASGAP-CAMKII	CAMKII-CAMKI	
	RASGAP-CALCIUM	CAMKII-RSK	
	RASGAP-AC2	CAMKK-CALCIUM	
	RASGAP-cAMP	CAMKK-AC2	
	PIP3-CAMKII	CAMKK-cAMP	
	PIP3-CALCIUM	NTYPECA-CALCIUM	
	ILK-CAMKII	AKT-CALCIUM	
	ILK-CALCIUM	AKT-AC2	
	ILK-AC2	AKT-cAMP	
	ILK-cAMP	CALCIUM-AC1	
	PDK1-CAMKII	CALCIUM-AC5	
	PDK1-CALCIUM	CALCIUM-AC2	
	PDK1-AC2	CALCIUM-cAMP	
	PDK1-cAMP	CALCIUM-GSK3	
	DAG-CAMKII	CALCIUM-CBP	
	DAG-CALCIUM	CALCIUM-CJUN	

Table S3.18. CREB activity level with two concurrently faulty molecules in the signaling network.

CREB Activity Level	Faulty Pairs of Molecules (Class 18)
2.625	PP2A-PDK1/ PP2A-RSK/ M2R-PP2B/ M4R-PP2B/ D3R-PP2B/ D1R-PP2B D2R-PP2B/ PP2B-NMDAR/ PP2B-MGLUR1/ PP2B-NTYPECA

Table S3.19. CREB activity level with two concurrently faulty molecules in the signaling network.

CREB Activity Level	Faulty Pairs of Molecules (Class 19)
2.598	PKC-PP2B/ PP2B-PI3K/ PP2B-PIP3

Table S3.20. CREB activity level with two concurrently faulty molecules in the signaling network.

CREB Activity Level	Faulty Pairs of Molecules (Class 20)			
2.583	PKC-CAMKIV	M4R-CREM	D2R-AC1	PP2B-CBP
	PKC-CREM	5HT1AR-PP2B	D2R-AC5	PP2B-CJUN
	PP2A-CAMKK	5HT2AR-PP2B	D2R-CAMKIV	PP2B-CAMKI
	PLCGAMMA-PP2B	5HT4R-PP2B	PP2B-GRB2	PP2B-RSK
	A1R-PP2B	D2R-CREM	PP2B-SAM68	NMDAR-CAMKIV
	A2AR-PP2B	PP2B-GALPHAS	PP2B-PLCBETA	NMDAR-CREM
	M1R-PP2B	D3R-AC1	PP2B-PIP2	MGLUR1-CAMKIV
	M2R-AC1	D3R-AC5	PP2B-RASGAP	MGLUR1-CREM
	M2R-AC5	D3R-CAMKIV	PP2B-ILK	PI3K-CAMKIV
	M2R-CAMKIV	D3R-CREM	PP2B-PDK1	PI3K-CREM
	M2R-CREM	D1R-AC1	PP2B-DAG	PIP3-CAMKIV
	M4R-AC1	D1R-AC5	PP2B-GALPHAZ	PIP3-CREM
	M4R-AC5	D1R-CAMKIV	PP2B-AKT	CAMKII-CAMKK
	M4R-CAMKIV	D1R-CREM	PP2B-GSK3	NTYPECA-CAMKIV
				NTYPECA-CREM

Table S3.21. CREB activity level with two concurrently faulty molecules in the signaling network.

CREB Activity Level	**Faulty Pairs of Molecules (Class 21)**
2.542	PP2B-CAMKK

Table S3.22. CREB activity level with two concurrently faulty molecules in the signaling network.

CREB Activity Level	Faulty Pairs of Molecules (Class 22)			
2.5	PLCGAMMA-AC1	5HT4R-AC5	PIP2-AC1	AKT-AC1
	PLCGAMMA-AC5	5HT4R-CAMKIV	PIP2-AC5	AKT-AC5
	PLCGAMMA-CAMKIV	5HT4R-CREM	PIP2-CAMKIV	AKT-CAMKIV
	PLCGAMMA-CREM	PP2B-MGLUR7	PIP2-CREM	AKT-CREM
	A1R-AC1	PP2B-CAMKIV	RASGAP-AC1	AC1-GSK3
	A1R-AC5	PP2B-CREM	RASGAP-AC5	AC1-CBP
	A1R-CAMKIV	MGLUR7-AC1	RASGAP-CAMKIV	AC1-CJUN
	A1R-CREM	MGLUR7-AC5	RASGAP-CREM	AC1-CAMKI
	A2AR-AC1	MGLUR7-CAMKIV	ILK-AC1	AC1-RSK
	A2AR-AC5	MGLUR7-CREM	ILK-AC5	AC5-GSK3
	A2AR-CAMKIV	GALPHAS-AC1	ILK-CAMKIV	AC5-CBP
	A2AR-CREM	GALPHAS-AC5	ILK-CREM	AC5-CJUN
	M1R-AC1	GALPHAS-CAMKIV	PDK1-AC1	AC5-CAMKI
	M1R-AC5	GALPHAS-CREM	PDK1-AC5	AC5-RSK
	M1R-CAMKIV	GRB2-AC1	PDK1-CAMKIV	GSK3-CAMKIV
	M1R-CREM	GRB2-AC5	PDK1-CREM	GSK3-CREM
	5HT1AR-AC1	GRB2-CAMKIV	DAG-AC1	CBP-CAMKIV
	5HT1AR-AC5	GRB2-CREM	DAG-AC5	CBP-CREM
	5HT1AR-CAMKIV	SAM68-AC1	DAG-CAMKIV	CJUN-CAMKIV
	5HT1AR-CREM	SAM68-AC5	DAG-CREM	CJUN-CREM
	5HT2AR-AC1	SAM68-CAMKIV	GALPHAZ-AC1	CAMKI-CAMKIV
	5HT2AR-AC5	SAM68-CREM	GALPHAZ-AC5	CAMKI-CREM
	5HT2AR-CAMKIV	PLCBETA-AC1	GALPHAZ-CAMKIV	CAMKIV-RSK
	5HT2AR-CREM	PLCBETA-AC5	GALPHAZ-CREM	CAMKIV-CREM
	5HT4R-AC1	PLCBETA-CAMKIV	CAMKK-CAMKIV	RSK-CREM
		PLCBETA-CREM	CAMKK-CREM	

Table S3.23. CREB activity level with two concurrently faulty molecules in the signaling network.

CREB Activity Level	Faulty Pairs of Molecules (Class 23)
2.458	CAMKK-AC1/ CAMKK-AC5

Table S3.24. CREB activity level with two concurrently faulty molecules in the signaling network.

CREB Activity Level	Faulty Pairs of Molecules (Class 24)
2.167	PP2A-GBETAGAMMA/ GALPHAI-GBETAGAMMA GBETAGAMMA-AC2/ GBETAGAMMA-cAMP

Table S3.25. CREB activity level with two concurrently faulty molecules in the signaling network.

CREB Activity Level	Faulty Pairs of Molecules (Class 25)
2.083	GBETAGAMMA-AC1/ GBETAGAMMA-AC5

Table S3.26. CREB activity level with two concurrently faulty molecules in the signaling network.

CREB Activity Level	Faulty Pairs of Molecules (Class 26)
1.917	PP2A-PP2B/ PP2B-CAMKII/ GBETAGAMMA-CAMKIV GBETAGAMMA-CREM

Table S3.27. CREB activity level with two concurrently faulty molecules in the signaling network.

CREB Activity Level	Faulty Pairs of Molecules (Class 27)	
1.833	PKA-PP2B	GALPHAI-CAMKIV
	PKA-CAMKIV	GALPHAI-CREM
	PKA-CREM	PQCaCh-CAMKIV
	CALMODULIN-PP2B	PQCaCh-CREM
	CALMODULIN-CAMKIV	CAMKII-CAMKIV
	CALMODULIN-CREM	CAMKII-CREM
	PP2A-CAMKIV	CALCIUM-CAMKIV
	PP2A-CREM	CALCIUM-CREM
	PP2B-GALPHAI	AC1-AC2
	PP2B-PQCaCh	AC5-AC2
	PP2B-CALCIUM	AC2-CAMKIV
	PP2B-AC2	AC2-CREM
	PP2B-cAMP	cAMP-CAMKIV
	GALPHAI-AC1	cAMP-CREM
	GALPHAI-AC5	

Table S3.28. CREB activity level with two concurrently faulty molecules in the signaling network.

CREB Activity Level	Faulty Pairs of Molecules (Class 28)
1.792	PP2B-GBETAGAMMA/ PP2B-AC1/ PP2B-AC5

Table S3.29. CREB activity level with two concurrently faulty molecules in the signaling network.

CREB Activity Level	Faulty Pairs of Molecules (Class 29)
1.75	AC1-AC5/ AC1-CAMKIV/ AC1-CREM/ AC5-CAMKIV/ AC5-CREM

Table S4. Vulnerability levels of all the individually faulty molecules of the CREB network.

Vulnerability Level	Faulty Molecules
0.6	PKA/ CALMODULIN/ PP2A/ GALPHAI/ PQCaCh/ CAMKII CALCIUM/ AC2/ cAMP
0.5	PP2B/ GBETAGAMMA/ AC1/ AC5/ CAMKIV/ CREM
0.2	A1R/ 5HT1AR/ MGLUR7
0.1	PKC/ M2R/ M4R/ D3R/ D1R/ D2R/ NMDAR/ MGLUR1 PI3K/ PIP3/ NTYPECA/ CAMKK
0	PLCGAMMA/ A2AR/ M1R/ 5HT2AR/ 5HT4R/ GALPHAS GRB2/ SAM68/ PLCBETA/ PIP2/ RASGAP/ ILK/ PDK1 DAG/ GALPHAZ/ AKT/ GSK3/ CBP/ CJUN/ CAMKI/ RSK

Table S5.1. All faulty pairs of molecules of the CREB network with vulnerability level of 0.8.

Vulnerability Level	Faulty Pairs of Molecules		
0.8	PKA-PP2B	PP2B-CALCIUM	CAMKII-CAMKIV
	PKA-CAMKIV	PP2B-AC2	CAMKII-CREM
	PKA-CREM	PP2B-cAMP	CALCIUM-CAMKIV
	CALMODULIN-PP2B	GALPHAI-GBETAGAMMA	CALCIUM-CREM
	CALMODULIN-CAMKIV	GALPHAI-AC1	AC1-AC2
	CALMODULIN-CREM	GALPHAI-AC5	AC5-AC2
	PP2A-PP2B	GALPHAI-CAMKIV	AC2-CAMKIV
	PP2A-CAMKIV	GALPHAI-CREM	AC2-CREM
	PP2A-CREM	GBETAGAMMA-AC2	cAMP-CAMKIV
	PP2B-GALPHAI	GBETAGAMMA-cAMP	cAMP-CREM
	PP2B-PQCaCh	PQCaCh-CREM	
	PP2B-CAMKII	PQCaCh-CAMKIV	

Table S5.2. All faulty pairs of molecules of the CREB network with vulnerability level of 0.75.

Vulnerability Level	Faulty Pairs of Molecules
0.75	PP2A-GBETAGAMMA/ PP2B-GBETAGAMMA/ PP2B-AC1
	PP2B-AC5/ GBETAGAMMA-AC1/ GBETAGAMMA-AC5
	GBETAGAMMA-CAMKIV/ GBETAGAMMA-CREM
	AC1-AC5/ AC1-CAMKIV/ AC1-CREM/ AC5-CAMKIV/ AC5-CREM

Table S5.3. All faulty pairs of molecules of the CREB network with vulnerability level of 0.6.

Vulnerability Level	Faulty Pairs of Molecules		
0.6	PKC-CALMODULIN	CALMODULIN-CJUN	CALMODULIN-CBP
	PKC-PP2A	CALMODULIN-CAMKI	5HT1AR-CALCIUM
	PKC-PQCaCh	CALMODULIN-RSK	5HT1AR-AC1
	PKC-CAMKII	PP2A-PLCGAMMA	5HT1AR-AC5
	PKC-CALCIUM	PP2A-A1R	5HT1AR-AC2
	PKA-CALMODULIN	PP2A-A2AR	5HT1AR-cAMP
	PKA-PP2A	PP2A-M1R	5HT1AR-CAMKIV
	PKA-PLCGAMMA	PP2A-M2R	5HT1AR-CREM
	PKA-A1R	PP2A-M4R	5HT2AR-GALPHAI
	PKA-A2AR	PP2A-5HT1AR	5HT2AR-PQCaCh
	PKA-M1R	PP2A-5HT2AR	5HT2AR-CAMKII
	PKA-M2R	PP2A-5HT4R	5HT2AR-CALCIUM
	PKA-M4R	PP2A-D3R	5HT2AR-AC2
	PKA-5HT1AR	PP2A-D1R	5HT2AR-cAMP
	PKA-5HT2AR	PP2A-D2R	5HT4R-GALPHAI
	PKA-5HT4R	PP2A-NMDAR	5HT4R-PQCaCh
	PKA-D3R	PP2A-MGLUR1	5HT4R-CAMKII
	PKA-D1R	PP2A-MGLUR7	5HT4R-CALCIUM
	PKA-D2R	PP2A-GALPHAI	5HT4R-AC2
	PKA-MGLUR1	PP2A-GALPHAS	5HT4R-cAMP
	PKA-MGLUR7	PP2A-PQCaCh	D3R-GALPHAI
	PKA-GALPHAI	PP2A-GRB2	D3R-PQCaCh
	PKA-GALPHAS	PP2A-SAM68	D3R-CAMKII
	PKA-GBETAGAMMA	PP2A-PLCBETA	D3R-CALCIUM
	PKA-PQCaCh	PP2A-PI3K	D3R-AC2
	PKA-GRB2	PP2A-PIP2	D3R-cAMP
	PKA-SAM68	PP2A-RASGAP	D1R-GALPHAI
	PKA-PLCBETA	PP2A-PIP3	D1R-PQCaCh
	PKA-PIP2	PP2A-ILK	D1R-CAMKII
	PKA-RASGAP	PP2A-PDK1	D1R-CALCIUM
	PKA-ILK	PP2A-DAG	D1R-AC2
	PKA-PDK1	PP2A-GALPHAZ	D1R-cAMP
	PKA-DAG	PP2A-CAMKII	D2R-GALPHAI
	PKA-GALPHAZ	PP2A-CAMKK	D2R-PQCaCh
	PKA-CAMKII	PP2A-NTYPECA	D2R-CAMKII
	PKA-CAMKK	PP2A-AKT	D2R-CALCIUM
	PKA-AKT	PP2A-CALCIUM	D2R-AC2
	PKA-CALCIUM	PP2A-AC1	D2R-cAMP
	PKA-AC1	PP2A-AC5	PP2B-MGLUR7
	PKA-AC5	PP2A-AC2	NMDAR-CAMKII
	PKA-AC2	PP2A-cAMP	MGLUR1-GALPHAI
	PKA-cAMP	PP2A-GSK3	MGLUR1-PQCaCh
	PKA-GSK3	PP2A-CBP	MGLUR1-CAMKII
	PKA-CBP	PP2A-CJUN	MGLUR1-CALCIUM
	PKA-CJUN	PP2A-CAMKI	MGLUR1-AC2
	PKA-CAMKI	PP2A-RSK	MGLUR1-cAMP
	PKA-RSK	PLCGAMMA-GALPHAI	MGLUR7-GALPHAI
	CALMODULIN-PP2A	PLCGAMMA-PQCaCh	

0.6	CALMODULIN-PLCGAMMA CALMODULIN-A1R CALMODULIN-A2AR CALMODULIN-M1R CALMODULIN-M2R CALMODULIN-M4R CALMODULIN-5HT1AR CALMODULIN-5HT2AR CALMODULIN-5HT4R CALMODULIN-D3R CALMODULIN-D1R CALMODULIN-D2R CALMODULIN-MGLUR1 CALMODULIN-MGLUR7 CALMODULIN-GALPHAI CALMODULIN-GALPHAS CALMODULIN-GBETAGAMMA CALMODULIN-PQCaCh CALMODULIN-GRB2 CALMODULIN-SAM68 CALMODULIN-PLCBETA CALMODULIN-PI3K CALMODULIN-PIP2 CALMODULIN-RASGAP CALMODULIN-PIP3 CALMODULIN-ILK CALMODULIN-PDK1 CALMODULIN-DAG CALMODULIN-GALPHAZ CALMODULIN-CAMKII CALMODULIN-CAMKK CALMODULIN-NTYPECA CALMODULIN-AKT CALMODULIN-CALCIUM CALMODULIN-AC1 CALMODULIN-AC5 CALMODULIN-AC2 CALMODULIN-cAMP CALMODULIN-GSK3 PQCaCh-PIP3 PQCaCh-ILK PQCaCh-PDK1 PQCaCh-DAG PQCaCh-GALPHAZ PQCaCh-CAMKII PQCaCh-CAMKK PQCaCh-AKT PQCaCh-CALCIUM PQCaCh-AC1 PQCaCh-AC5	PLCGAMMA-CAMKII PLCGAMMA-CALCIUM PLCGAMMA-AC2 PLCGAMMA-cAMP A1R-PP2B A1R-GALPHAI A1R-GBETAGAMMA A1R-PQCaCh A1R-CAMKII A1R-CALCIUM A1R-AC1 A1R-AC5 A1R-AC2 A1R-cAMP A1R-CAMKIV A1R-CREM A2AR-GALPHAI A2AR-PQCaCh A2AR-CAMKII A2AR-CALCIUM A2AR-AC2 A2AR-cAMP M1R-GALPHAI M1R-PQCaCh M1R-CAMKII M1R-CALCIUM M1R-AC2 M1R-cAMP M2R-GALPHAI M2R-PQCaCh M2R-CAMKII M2R-CALCIUM M2R-AC2 M2R-cAMP M4R-GALPHAI M4R-PQCaCh M4R-CAMKII M4R-CALCIUM M4R-AC2 M4R-cAM RASGAP-CALCIUM RASGAP-AC2 RASGAP-cAMP PIP3-CAMKII PIP3-CALCIUM ILK-CAMKII ILK-CALCIUM ILK-AC2 ILK-cAMP PDK1-CAMKII PDK1-CALCIUM	MGLUR7-GBETAGAMMA MGLUR7-PQCaCh MGLUR7-CAMKII MGLUR7-CALCIUM MGLUR7-AC1 MGLUR7-AC5 MGLUR7-AC2 MGLUR7-cAMP MGLUR7-CAMKIV MGLUR7-CREM GALPHAI-GALPHAS GALPHAI-PQCaCh GALPHAI-GRB2 GALPHAI-SAM68 GALPHAI-PLCBETA GALPHAI-PIP2 GALPHAI-RASGAP GALPHAI-ILK GALPHAI-PDK1 GALPHAI-DAG GALPHAI-GALPHAZ GALPHAI-CAMKII GALPHAI-CAMKK GALPHAI-AKT GALPHAI-CALCIUM GALPHAI-AC2 GALPHAI-cAMP GALPHAI-GSK3 GALPHAI-CBP GALPHAI-CJUN GALPHAI-CAMKI GALPHAI-RSK GALPHAS-PQCaCh GALPHAS-CAMKII GALPHAS-CALCIUM GALPHAS-AC2 GALPHAS-cAMP GBETAGAMMA-PQCaCh GBETAGAMMA-CAMKII GBETAGAMMA-CALCIUM PQCaCh-GRB2 AKT-cAMP CALCIUM-AC1 CALCIUM-AC5 CALCIUM-AC2 CALCIUM-cAMP CALCIUM-GSK3

0.6	PQCaCh-AC2 PQCaCh-cAMP PQCaCh-GSK3 PQCaCh-CBP PQCaCh-CJUN PQCaCh-CAMKI PQCaCh-RSK GRB2-CAMKII GRB2-CALCIUM GRB2-AC2 GRB2-cAMP SAM68-CAMKII SAM68-CALCIUM SAM68-AC2 SAM68-cAMP PLCBETA-CAMKII PLCBETA-CALCIUM PLCBETA-AC2 PLCBETA-cAMP PI3K-CAMKII PI3K-CALCIUM PIP2-CAMKII PIP2-CALCIUM PIP2-AC2 PIP2-cAMP RASGAP-CAMKII	PDK1-AC2 PDK1-cAMP DAG-CAMKII DAG-CALCIUM DAG-AC2 DAG-cAMP GALPHAZ-CAMKII GALPHAZ-CALCIUM GALPHAZ-AC2 GALPHAZ-cAMP CAMKII-CAMKK CAMKII-NTYPECA CAMKII-AKT CAMKII-CALCIUM CAMKII-AC1 CAMKII-AC5 CAMKII-AC2 CAMKII-cAMP CAMKII-GSK3 CAMKII-CBP CAMKII-CJUN CAMKII-CAMKI CAMKII-RSK CAMKK-CALCIUM CAMKK-AC2 CAMKK-cAMP NTYPECA-CALCIUM AKT-CALCIUM AKT-AC2	CALCIUM-CBP CALCIUM-CJUN AC2-CAMKI AC2-RSK cAMP-GSK3 cAMP-CBP cAMP-CJUN cAMP-CAMKI cAMP-RSK 5HT1AR-PP2B 5HT1AR-GALPHAI 5HT1AR-GBETAGAMMA 5HT1AR-PQCaCh 5HT1AR-CAMKII PQCaCh-SAM68 PQCaCh-PLCBETA PQCaCh-PI3K PQCaCh-PIP2 PQCaCh-RASGAP CALCIUM-CAMKI CALCIUM-RSK AC1-cAMP AC5-cAMP AC2-cAMP AC2-GSK3 AC2-CBP AC2-CJUN

Table S5.4. All faulty pairs of molecules of the CREB network with vulnerability level of 0.55.

Vulnerability Level	Faulty Pairs of Molecules		
0.55	PKC-CAMKIV	D3R-AC5	PP2B-NTYPECA
	PKC-CREM	D3R-CAMKIV	NMDAR-CAMKIV
	M2R-PP2B	D3R-CREM	NMDAR-CREM
	M2R-GBETAGAMMA	D1R-PP2B	MGLUR1-AC1
	M2R-AC1	D1R-GBETAGAMMA	MGLUR1-AC5
	M2R-AC5	D1R-AC1	MGLUR1-CAMKIV
	M2R-CAMKIV	D1R-AC5	MGLUR1-CREM
	M2R-CREM	D1R-CAMKIV	GBETAGAMMA-CAMKK
	M4R-PP2B	D1R-CREM	PI3K-CAMKIV
	M4R-GBETAGAMMA	D2R-PP2B	PI3K-CREM
	M4R-AC1	D2R-GBETAGAMMA	PIP3-CAMKIV
	M4R-AC5	D2R-AC1	PIP3-CREM
	M4R-CAMKIV	D2R-AC5	CAMKK-AC1
	M4R-CREM	D2R-CAMKIV	CAMKK-AC5
	D3R-PP2B	D2R-CREM	NTYPECA-CAMKIV
	D3R-GBETAGAMMA	PP2B-NMDAR	NTYPECA-CREM
	D3R-AC1	PP2B-MGLUR1	

Table S5.5. All faulty pairs of molecules of the CREB network with vulnerability level of 0.5.

Vulnerability Level	Faulty Pairs of Molecules		
0.5	PKC-PP2B	GBETAGAMMA-RASGAP	CAMKK-CAMKIV
	PLCGAMMA-PP2B	GBETAGAMMA-ILK	CAMKK-CREM
	PLCGAMMA-AC1	GBETAGAMMA-GALPHAZ	AKT-AC1
	PLCGAMMA-AC5	GBETAGAMMA-AKT	AKT-AC5
	PLCGAMMA-CAMKIV	GBETAGAMMA-GSK3	AKT-CAMKIV
	PLCGAMMA-CREM	GBETAGAMMA-CBP	AKT-CREM
	A2AR-PP2B	GBETAGAMMA-CJUN	AC1-GSK3
	A2AR-GBETAGAMMA	GBETAGAMMA-CAMKI	AC1-CBP
	A2AR-AC1	GBETAGAMMA-RSK	AC1-CJUN
	A2AR-AC5	GRB2-AC1	AC1-CAMKI
	A2AR-CAMKIV	GRB2-AC5	AC1-RSK
	A2AR-CREM	GRB2-CAMKIV	AC5-GSK3
	M1R-PP2B	GRB2-CREM	AC5-CBP
	M1R-GBETAGAMMA	SAM68-AC1	AC5-CJUN
	M1R-AC1	SAM68-AC5	AC5-CAMKI
	M1R-AC5	SAM68-CAMKIV	AC5-RSK
	M1R-CAMKIV	SAM68-CREM	GSK3-CAMKIV
	M1R-CREM	PLCBETA-AC1	GSK3-CREM
	5HT2AR-PP2B	PLCBETA-AC5	CBP-CAMKIV
	5HT2AR-GBETAGAMMA	PLCBETA-CAMKIV	CBP-CREM
	5HT2AR-AC1	PLCBETA-CREM	CJUN-CAMKIV
	5HT2AR-AC5	PIP2-AC1	CJUN-CREM
	5HT2AR-CAMKIV	PIP2-AC5	CAMKI-CAMKIV
	5HT2AR-CREM	PIP2-CAMKIV	CAMKI-CREM
	5HT4R-PP2B	PIP2-CREM	CAMKIV-RSK
	5HT4R-GBETAGAMMA	RASGAP-AC1	CAMKIV-CREM
	5HT4R-AC1	RASGAP-AC5	RSK-CREM
	5HT4R-AC5	RASGAP-CAMKIV	RASGAP-CREM
	5HT4R-CAMKIV		ILK-AC1

	5HT4R-CREM	PP2B-CJUN	ILK-CREM
	PP2B-GALPHAS	PP2B-CAMKI	PDK1-AC1
	PP2B-GRB2	PP2B-CAMKIV	PDK1-AC5
	PP2B-SAM68	PP2B-RSK	PDK1-CAMKIV
	PP2B-PLCBETA	PP2B-CREM	PDK1-CREM
	PP2B-PI3K	MGLUR1-GBETAGAMMA	DAG-AC1
	PP2B-PIP2	GALPHAS-GBETAGAMMA	DAG-AC5
	PP2B-RASGAP		DAG-CAMKIV
	PP2B-PIP3	GALPHAS-AC1	DAG-CREM
	PP2B-ILK	GALPHAS-AC5	GALPHAZ-AC1
	PP2B-PDK1	GALPHAS-CAMKIV	GALPHAZ-AC5
	PP2B-DAG	GALPHAS-CREM	GALPHAZ-CAMKIV
	PP2B-GALPHAZ	GBETAGAMMA-GRB2	GALPHAZ-CREM
	PP2B-CAMKK	GBETAGAMMA-SAM68	
	PP2B-AKT	GBETAGAMMA-PIP2	
	PP2B-GSK3	ILK-AC5	
	PP2B-CBP	ILK-CAMKIV	

Table S5.6. All faulty pairs of molecules of the CREB network with vulnerability level of 0.4.

Vulnerability Level	**Faulty Pairs of Molecules**		
0.4	PKC-PKA	NMDAR-GALPHAI	PQCaCh-NTYPECA
	PKC-GALPHAI	NMDAR-PQCaCh	PI3K-AC2
	PKC-AC2	NMDAR-CALCIUM	PI3K-cAMP
	PKC-cAMP	NMDAR-AC2	PIP3-AC2
	PKA-NMDAR	NMDAR-cAMP	PIP3-cAMP
	PKA-PI3K	GALPHAI-PI3K	NTYPECA-AC2
	PKA-PIP3	GALPHAI-PIP3	NTYPECA-cAMP
	PKA-NTYPECA	GALPHAI-NTYPECA	
	CALMODULIN-NMDAR		

Table S5.7. All faulty pairs of molecules of the CREB network with vulnerability level of 0.35.

Vulnerability Level	Faulty Pairs of Molecules	
0.35	PKC-GBETAGAMMA	PI3K-AC1
	PKC-AC1	PI3K-AC5
	PKC-AC5	PIP3-AC1
	NMDAR-GBETAGAMMA	PIP3-AC5
	NMDAR-AC1	NTYPECA-AC1
	NMDAR-AC5	NTYPECA-AC5
	GBETAGAMMA-PI3K	
	GBETAGAMMA-PIP3	
	GBETAGAMMA-NTYPECA	

Table S5.8. All faulty pairs of molecules of the CREB network with vulnerability level of 0.3.

Vulnerability Level	Faulty Pairs of Molecules
0.3	PLCGAMMA-GBETAGAMMA/ GBETAGAMMA-PLCBETA
	GBETAGAMMA-PDK1/ GBETAGAMMA-DAG

Table S5.9. All faulty pairs of molecules of the CREB network with vulnerability level of 0.25.

Vulnerability Level	Faulty Pairs of Molecules
0.25	A1R-5HT1AR/ A1R-MGLUR1/ A1R-MGLUR7/ A1R-CAMKK
	5HT1AR-MGLUR1/ 5HT1AR-MGLUR7/ 5HT1AR-CAMKK

Table S5.10. All faulty pairs of molecules of the CREB network with vulnerability level of 0.2.

Vulnerability Level	Faulty Pairs of Molecules		
0.2	PKC-A1R	A1R-DAG	MGLUR7-ILK
	PKC-5HT1AR	A1R-GALPHAZ	MGLUR7-PDK1
	PKC-MGLUR7	M1R-5HT1AR	MGLUR7-DAG
	PLCGAMMA-A1R	M1R-MGLUR7	MGLUR7-GALPHAZ
	PLCGAMMA-5HT1AR	M2R-M4R	5HT1AR-PLCBETA
	PLCGAMMA-MGLUR7	M2R-5HT1AR	5HT1AR-PI3K
	A1R-A2AR	M2R-MGLUR7	5HT1AR-PIP2
	A1R-M1R	M4R-5HT1AR	5HT1AR-RASGAP
	A1R-M2R	M4R-MGLUR7	5HT1AR-PIP3
	A1R-M4R	MGLUR7-CAMKK	5HT1AR-ILK
	A1R-5HT2AR	MGLUR7-NTYPECA	5HT1AR-PDK1
	A1R-5HT4R	MGLUR7-AKT	5HT1AR-DAG
	A1R-D3R	MGLUR7-GSK3	5HT1AR-GALPHAZ
	A1R-D1R	MGLUR7-CBP	5HT1AR-NTYPECA
	A1R-D2R	MGLUR7-CJUN	5HT1AR-AKT
	A1R-NMDAR	MGLUR7-CAMKI	5HT1AR-GSK3
	A1R-GALPHAS	MGLUR7-RSK	5HT1AR-CBP
	A1R-GRB2	MGLUR1-MGLUR7	5HT1AR-CJUN
	A1R-SAM68	MGLUR7-GALPHAS	5HT1AR-CAMKI
	A1R-PLCBETA	MGLUR7-GRB2	5HT1AR-RSK
	A1R-PI3K	MGLUR7-SAM68	5HT2AR-MGLUR7
	A1R-PIP2	MGLUR7-PLCBETA	5HT4R-MGLUR7
	A1R-RASGAP	MGLUR7-PI3K	D3R-MGLUR7
	A1R-PIP3	MGLUR7-PIP2	D1R-MGLUR7
	A1R-ILK	MGLUR7-RASGAP	D2R-MGLUR7
	A1R-PDK1	MGLUR7-PIP3	NMDAR-MGLUR7
	A1R-NTYPECA	5HT1AR-5HT2AR	5HT1AR-GALPHAS
	A1R-AKT	5HT1AR-5HT4R	5HT1AR-GRB2

0.2	A1R-GSK3	A2AR-MGLUR7	5HT1AR-D1R
	A1R-CBP	A1R-CAMKI	5HT1AR-D2R
	A1R-CJUN	A1R-RSK	5HT1AR-NMDAR
	A2AR-5HT1AR	5HT1AR-D3R	5HT1AR-SAM68

Table S5.11. All faulty pairs of molecules of the CREB network with vulnerability level of 0.15.

Vulnerability Level	**Faulty Pairs of Molecules**		
0.15	PKC-M2R	D1R-NMDAR	M4R-D2R
	PKC-M4R	D1R-MGLUR1	M4R-NMDAR
	PKC-D3R	D1R-PI3K	M4R-MGLUR1
	PKC-D1R	D1R-PIP3	M4R-PI3K
	PKC-D2R	D1R-CAMKK	M4R-PIP3
	PKC-MGLUR1	D1R-NTYPECA	M4R-CAMKK
	PKC-CAMKK	D2R-NMDAR	M4R-NTYPECA
	PKC-NTYPECA	D2R-MGLUR1	D3R-D1R
	M2R-D3R	D2R-PI3K	D3R-D2R
	M2R-D1R	D2R-PIP3	D3R-NMDAR
	M2R-D2R	D2R-CAMKK	D3R-MGLUR1
	M2R-NMDAR	D2R-NTYPECA	D3R-PI3K
	M2R-MGLUR1	NMDAR-MGLUR1	D3R-PIP3
	M2R-PI3K	NMDAR-CAMKK	D3R-CAMKK
	M2R-PIP3	NMDAR-NTYPECA	D3R-NTYPECA
	M2R-CAMKK	MGLUR1-PI3K	PI3K-NTYPECA
	M2R-NTYPECA	MGLUR1-PIP3	PIP3-CAMKK
	M4R-D3R	MGLUR1-CAMKK	PIP3-NTYPECA
	M4R-D1R	MGLUR1-NTYPECA	CAMKK-NTYPECA
	D1R-D2R	PI3K-CAMKK	

Table S5.12. All faulty pairs of molecules of the CREB network with vulnerability level of 0.1.

Vulnerability Level	Faulty Pairs of Molecules		
0.1	PKC-PLCGAMMA	M4R-AKT	NMDAR-GSK3
	PKC-A2AR	M4R-GSK3	NMDAR-CBP
	PKC-M1R	M4R-CBP	NMDAR-CJUN
	PKC-5HT2AR	M4R-CJUN	NMDAR-CAMKI
	PKC-5HT4R	M4R-CAM	NMDAR-RSK
	PKC-NMDAR	M4R-RSK	MGLUR1-GALPHAS
	PKC-GALPHAS	5HT2AR-D3R	MGLUR1-GRB2
	PKC-GRB2	5HT2AR-D1R	MGLUR1-SAM68
	PKC-SAM68	5HT2AR-D2R	MGLUR1-PLCBETA
	PKC-PLCBETA	5HT2AR-NMDAR	MGLUR1-PIP2
	PKC-PI3K	5HT2AR-PI3K	MGLUR1-AKT
	PKC-PIP2	5HT2AR-PIP3	MGLUR1-GSK3
	PKC-RASGAP	5HT2AR-CAMKK	MGLUR1-CBP
	PKC-PIP3	5HT2AR-NTYPECA	MGLUR1-CJUN
	PKC-ILK	5HT4R-D3R	MGLUR1-CAMKI
	PKC-PDK1	5HT4R-D1R	MGLUR1-RSK
	PKC-DAG	5HT4R-D2R	GALPHAS-PI3K
	PKC-GALPHAZ	5HT4R-NMDAR	GALPHAS-PIP3
	PKC-AKT	5HT4R-PI3K	GALPHAS-CAMKK
	PKC-GSK3	5HT4R-PIP3	GALPHAS-NTYPECA
	PKC-CBP	5HT4R-CAMKK	GRB2-PI3K
	PKC-CJUN	5HT4R-NTYPECA	GRB2-PIP3
	PKC-CAMKI	D3R-GALPHAS	GRB2-CAMKK
	PKC-RSK	D3R-GRB2	GRB2-NTYPECA
	PLCGAMMA-M2R	D3R-SAM68	SAM68-PI3K
	PLCGAMMA-M4R	D3R-PLCBETA	SAM68-PIP3
	PLCGAMMA-D3R	D3R-PIP2	SAM68-CAMKK
	PLCGAMMA-D1R	D3R-RASGAP	SAM68-NTYPECA
	PLCGAMMA-D2R	D3R-ILK	PLCBETA-CAMKK
	PLCGAMMA-NMDAR	D3R-PDK1	PLCBETA-NTYPECA

0.1	PLCGAMMA-MGLUR1	D3R-DAG	PI3K-PIP2
	PLCGAMMA-CAMKK	D3R-GALPHAZ	PI3K-RASGAP
	PLCGAMMA-NTYPECA	D3R-AKT	PI3K-PIP3
	A2AR-M2R	D3R-GSK3	PI3K-ILK
	A2AR-M4R	D3R-CBP	PI3K-GALPHAZ
	A2AR-D3R	D3R-CJUN	PI3K-AKT
	A2AR-D1R	D3R-CAMKI	PI3K-GSK3
	A2AR-D2R	D3R-RSK	PI3K-CBP
	A2AR-NMDAR	D1R-GALPHAS	PI3K-CJUN
	A2AR-PI3K	D1R-GRB2	PI3K-CAMKI
	A2AR-PIP3	D1R-SAM68	PI3K-RSK
	A2AR-CAMKK	D1R-PLCBETA	PIP2-PIP3
	A2AR-NTYPECA	D1R-PIP2	PIP2-CAMKK
	M1R-M2R	D1R-RASGAP	PIP2-NTYPECA
	M1R-M4R	D1R-ILK	RASGAP-PIP3
	M1R-D3R	D1R-PDK1	RASGAP-CAMKK
	M1R-D1R	D1R-DAG	RASGAP-NTYPECA
	M1R-D2R	D1R-GALPHAZ	PIP3-ILK
	M1R-NMDAR	D1R-AKT	PIP3-GALPHAZ
	M1R-PI3K	D1R-GSK3	PIP3-AKT
	M1R-PIP3	D1R-CBP	PIP3-GSK3
	M1R-CAMKK	D1R-CJUN	PIP3-CBP
	M1R-NTYPECA	D1R-CAMKI	PIP3-CJUN
	M2R-5HT2AR	D1R-RSK	PIP3-CAMKI
	M2R-5HT4R	D2R-GALPHAS	PIP3-RSK
	M2R-GALPHAS	D2R-GRB2	ILK-CAMKK
	M2R-GRB2	D2R-SAM68	ILK-NTYPECA
	M2R-SAM68	D2R-PLCBETA	PDK1-CAMKK
	M2R-PLCBETA	D2R-PIP2	PDK1-NTYPECA
	M2R-PIP2	D2R-RASGAP	DAG-CAMKK
	M2R-RASGAP	D2R-ILK	DAG-NTYPECA
	M2R-ILK	D2R-PDK1	GALPHAZ-CAMKK

0.1	M2R-PDK1	D2R-DAG	GALPHAZ-NTYPECA
	M2R-DAG	D2R-GALPHAZ	CAMKK-AKT
	M2R-GALPHAZ	D2R-AKT	CAMKK-GSK3
	M2R-AKT	D2R-GSK3	CAMKK-CBP
	M2R-GSK3	D2R-CBP	CAMKK-CJUN
	M2R-CBP	D2R-CJUN	CAMKK-CAMKI
	M2R-CJUN	D2R-CAMKI	CAMKK-RSK
	M2R-CAMKI	D2R-RSK	NTYPECA-AKT
	M2R-RSK	NMDAR-GALPHAS	NTYPECA-GSK3
	M4R-5HT2AR	NMDAR-GRB2	NTYPECA-CBP
	M4R-5HT4R	NMDAR-SAM68	NTYPECA-CJUN
	M4R-GALPHAS	NMDAR-PLCBETA	NTYPECA-CAMKI
	M4R-GRB2	NMDAR-PI3K	NTYPECA-RSK
	M4R-SAM68	NMDAR-PIP2	MGLUR1-RASGAP
	M4R-PLCBETA	NMDAR-RASGAP	MGLUR1-ILK
	M4R-PIP2	NMDAR-PIP3	MGLUR1-PDK1
	M4R-RASGAP	NMDAR-ILK	MGLUR1-DAG
	M4R-ILK	NMDAR-PDK1	MGLUR1-GALPHAZ
	M4R-PDK1	NMDAR-DAG	
	M4R-DAG	NMDAR-GALPHAZ	
	M4R-GALPHAZ	NMDAR-AKT	

Table S5.13. All faulty pairs of molecules of the CREB network with vulnerability level of 0.05.

Vulnerability Level	**Faulty Pairs of Molecules**
0.05	PLCGAMMA-PI3K/ PLCGAMMA-PIP3/ A2AR-MGLUR1
	M1R-MGLUR1/ 5HT2AR-MGLUR1/ 5HT4R-MGLUR1
	PLCBETA-PI3K/ PLCBETA-PIP3/ PI3K-PDK1
	PI3K-DAG/ PIP3-PDK1/ PIP3-DAG

Table S5.14. All faulty pairs of molecules of the CREB network with vulnerability level of 0.

Vulnerability Level	Faulty Pairs of Molecules		
0	PLCGAMMA-A2AR	5HT2AR-CBP	PIP2-RASGAP
	PLCGAMMA-M1R	5HT2AR-CJUN	PIP2-ILK
	PLCGAMMA-5HT2AR	5HT2AR-CAMKI	PIP2-PDK1
	PLCGAMMA-5HT4R	5HT2AR-RSK	PIP2-DAG
	PLCGAMMA-GALPHAS	5HT4R-GALPHAS	PIP2-GALPHAZ
	PLCGAMMA-GRB2	5HT4R-GRB2	PIP2-AKT
	PLCGAMMA-SAM68	5HT4R-SAM68	PIP2-GSK3
	PLCGAMMA-PLCBETA	5HT4R-PLCBETA	PIP2-CBP
	PLCGAMMA-PIP2	5HT4R-PIP2	PIP2-CJUN
	PLCGAMMA-RASGAP	5HT4R-RASGAP	PIP2-CAMKI
	PLCGAMMA-ILK	5HT4R-ILK	PIP2-RSK
	PLCGAMMA-PDK1	5HT4R-PDK1	RASGAP-ILK
	PLCGAMMA-DAG	5HT4R-DAG	RASGAP-PDK1
	PLCGAMMA-GALPHAZ	5HT4R-GALPHAZ	RASGAP-DAG
	PLCGAMMA-AKT	5HT4R-AKT	RASGAP-GALPHAZ
	PLCGAMMA-GSK3	5HT4R-GSK3	RASGAP-AKT
	PLCGAMMA-CBP	5HT4R-CBP	RASGAP-GSK3
	PLCGAMMA-CJUN	5HT4R-CJUN	RASGAP-CBP
	PLCGAMMA-CAMKI	5HT4R-CAMKI	RASGAP-CJUN
	PLCGAMMA-RSK	5HT4R-RSK	RASGAP-CAMKI
	A2AR-M1R	GALPHAS-GRB2	RASGAP-RSK
	A2AR-5HT2AR	GALPHAS-SAM68	ILK-PDK1
	A2AR-5HT4R	GALPHAS-PLCBETA	ILK-DAG
	A2AR-GALPHAS	GALPHAS-PIP2	ILK-GALPHAZ
	A2AR-GRB2	GALPHAS-RASGAP	ILK-AKT
	A2AR-SAM68	GALPHAS-ILK	ILK-GSK3
	A2AR-PLCBETA	GALPHAS-PDK1	ILK-CBP
	A2AR-PIP2	GALPHAS-DAG	ILK-CJUN

0	A2AR-RASGAP	GALPHAS-GALPHAZ	ILK-CAMKI
	A2AR-ILK	GALPHAS-AKT	ILK-RSK
	A2AR-PDK1	GALPHAS-GSK3	PDK1-DAG
	A2AR-DAG	GALPHAS-CBP	PDK1-GALPHAZ
	A2AR-GALPHAZ	GALPHAS-CJUN	PDK1-AKT
	A2AR-AKT	GALPHAS-CAMKI	PDK1-GSK3
	A2AR-GSK3	GALPHAS-RSK	PDK1-CBP
	A2AR-CBP	GRB2-SAM68	PDK1-CJUN
	A2AR-CJUN	GRB2-PLCBETA	PDK1-CAMKI
	A2AR-CAMKI	GRB2-PIP2	PDK1-RSK
	A2AR-RSK	GRB2-RASGAP	DAG-GALPHAZ
	M1R-5HT2AR	GRB2-ILK	DAG-AKT
	M1R-5HT4R	GRB2-PDK1	DAG-GSK3
	M1R-GALPHAS	GRB2-DAG	DAG-CBP
	M1R-GRB2	GRB2-GALPHAZ	DAG-CJUN
	M1R-SAM68	GRB2-AKT	DAG-CAMKI
	M1R-PLCBETA	GRB2-GSK3	DAG-RSK
	M1R-PIP2	GRB2-CBP	GALPHAZ-AKT
	M1R-RASGAP	GRB2-CJUN	GALPHAZ-GSK3
	M1R-ILK	GRB2-CAMKI	GALPHAZ-CBP
	M1R-PDK1	GRB2-RSK	GALPHAZ-CJUN
	M1R-DAG	SAM68-PLCBETA	GALPHAZ-CAMKI
	M1R-GALPHAZ	SAM68-PIP2	GALPHAZ-RSK
	M1R-AKT	SAM68-RASGAP	AKT-GSK3
	M1R-GSK3	SAM68-ILK	AKT-CBP
	M1R-CBP	SAM68-PDK1	AKT-CJUN
	M1R-CJUN	SAM68-DAG	AKT-CAMKI
	M1R-CAMKI	SAM68-GALPHAZ	AKT-RSK
	M1R-RSK	SAM68-AKT	GSK3-CBP
	5HT2AR-5HT4R	SAM68-GSK3	GSK3-CJUN
	5HT2AR-GALPHAS	SAM68-CBP	GSK3-CAMKI
	5HT2AR-GRB2	SAM68-CJUN	GSK3-RSK

0	5HT2AR-SAM68	SAM68-CAMKI	CBP-CJUN
	5HT2AR-PLCBETA	SAM68-RSK	CBP-CAMKI
	5HT2AR-PIP2	PLCBETA-PIP2	CBP-RSK
	5HT2AR-RASGAP	PLCBETA-RASGAP	CJUN-CAMKI
	5HT2AR-ILK	PLCBETA-ILK	CJUN-RSK
	5HT2AR-PDK1	PLCBETA-PDK1	CAMKI-RSK
	5HT2AR-DAG	PLCBETA-DAG	PLCBETA-CBP
	5HT2AR-GALPHAZ	PLCBETA-GALPHAZ	PLCBETA-CJUN
	5HT2AR-AKT	PLCBETA-AKT	PLCBETA-CAMKI
	5HT2AR-GSK3	PLCBETA-GSK3	PLCBETA-RSK

Table S6. Numerical values and molecular class labels for the data points of Figure 6B.

Vulnerability Level	Normalized Neuronal Activity	Class No.
0.8	0.554	24
	0.498	26
	0.481	27
0.75	0.554	24
	0.534	25
	0.498	26
	0.471	28
	0.461	29
0.6	0.702	14
	0.662	17
	0.653	18
	0.645	20
	0.630	22
0.55	0.715	13
	0.690	15
	0.680	16
	0.653	18
	0.645	20
	0.616	23
0.5	0.702	14
	0.647	19
	0.634	21
	0.630	22
0.4	0.864	9
	0.822	11
0.35	0.879	8
	0.841	10

	0.802	12
0.3	0.864	9
0.25	1.021	4
	1	6
	0.982	7
0.2	1.051	2
	1	6
	0.982	7
0.15	1.073	1
	1.035	3
	1.025	5
0.1	1.051	2
	0.982	7
0.05	1.021	4
0	1	6

Table S7. Numerical values and molecular class labels for the data points of Figure 8B.

Vulnerability Level	Normalized Synaptic Weight	Class No.
0.8	0.827	27
	0.703	24
	0.591	26
0.75	0.858	28
	0.843	29
	0.703	24
	0.654	25
	0.591	26
0.6	0.707	22
	0.705	17, 14
	0.688	18
0.55	0.726	15
	0.723	13
	0.704	23
	0.702	16
	0.688	18
	0.687	20
0.5	0.707	22
	0.705	14
	0.700	21
	0.687	20
	0.678	19
0.4	0.873	9
	0.863	11
0.35	0.928	8
	0.898	10

	0.852	12
0.3	0.873	9
0.25	1.082	4
	1.034	7
	1	6
0.2	1.114	2
	1.034	7
	1	6
0.15	1.298	1
	1.096	5
	1.083	3
0.1	1.114	2
	1.034	7
0.05	1.082	4
0	1	6

SUPPLEMENTARY REFERENCES

1. De Vivo, M. & Maayani, S. Characterization of the 5-hydroxytryptamine1a receptor-mediated inhibition of forskolin-stimulated adenylate cyclase activity in guinea pig and rat hippocampal membranes. J. Pharmacol. Exp. Ther. 238, 248 (1986).
2. Barr, A. J. & Manning, D. R. Agonist-independent activation of Gz by the 5-hydroxytryptamine1A receptor co-expressed in Spodoptera frugiperda cells. Distinguishing inverse agonists from neutral antagonists. J. Biol. Chem. 272, 32979 (1998).
3. Conn, P. J. & Sanders-Bush, E. Selective 5HT-2 antagonists inhibit serotonin stimulated phosphatidylinositol metabolism in cerebral cortex. Neuropharmacology 23, 993 (1984).
4. Bockaert, J. et al. Pharmacological characterization of 5-hydroxytryptamine4(5-HT4) receptors positively coupled to adenylate cyclase in adult guinea pig hippocampal membranes: effect of substituted benzamide derivatives. Mol. Pharmacol. 37, 408 (1990).
5. Cooper, D. M. et al. Adenosine receptor-mediated inhibition of rat cerebral cortical adenylate cyclase by a GTP-dependent process. Mol. Pharmacol. 18, 598 (1981).
6. Olah, M. E. Identification of A2a adenosine receptor domains involved in selective coupling to Gs. Analysis of chimeric A1/A2a adenosine receptors. J. Biol. Chem. 272, 337 (1997).
7. Tang, W. J. et al. Expression and characterization of calmodulin-activated (type I) adenylylcyclase. J. Biol. Chem. 266, 8595 (1991).
8. Evan, G. I. & Vousden, K. H. Proliferation, cell cycle and apoptosis in cancer. Nature. 411, 342 (2001).
9. Ishikawa, Y. et al. Isolation and characterization of a novel cardiac adenylylcyclase cDNA. J. Biol. Chem. 267, 13553 (1992).
10. Berstein, G. et al. Reconstitution of agonist-stimulated phosphatidylinositol 4,5-bisphosphate hydrolysis using purified m1 muscarinic receptor, Gq/11, and phospholipase C-beta 1. J. Biol. Chem. 267, 8081 (1992).
11. Bonner, T. I. et al. Identification of a family of muscarinic acetylcholine receptor genes. Science. 237, 527 (1987).
12. van Koppen, C. J. et al. Isolation, sequence and functional expression of the mouse m4 muscarinic acetylcholine receptor gene. Biochim. Biophys. Acta. 1173, 342 (1993).
13. Libert, F. et al. Selective amplification and cloning of four new members of the G protein-coupled receptor family. Science. 244, 569 (1989).
14. Cross, D. A. et al. Inhibition of glycogen synthase kinase-3 by insulin mediated by protein kinase B. Nature. 378, 785 (1996).
15. Hu, B. et al. A critical interplay between Ca^{2+} inhibition and activation by Mg^{2+} of AC5 revealed by mutants and chimeric constructs. J. Biol. Chem. 277, 33139 (2002).
16. Watterson, D. M. et al. The complete amino acid sequence of the Ca^{2+}- dependent modulator protein (calmodulin) of bovine brain. J. Biol. Chem. 255, 962 (1980).
17. Takai, Y. et al. Calcium-dependent activation of a multifunctional protein kinase by membrane phospholipids. J. Biol. Chem. 254, 3692 (1979).
18. Xia, Z. et al. Type I calmodulin-sensitive adenylyl cyclase is neural specific. J. Neurochem. 60, 305 (1993).

19. Miller, S. G. & Kennedy, M. B. Regulation of brain type II Ca^{2+}/calmodulindependent protein kinase by autophosphorylation: a Ca^{2+}-triggered molecular switch. Cell. 44, 861 (1986).

20. Kameshita, I. & Fujisawa, H. Autophosphorylation of calmodulin-dependent protein kinase IV from rat cerebral cortex. J. Biochem. (Tokyo). 113, 583 (1993).

21. Matsushita, M. & Nairn, A. C. Inhibition of the Ca^{2+}/calmodulin-dependent protein kinase I cascade by cAMP-dependent protein kinase. J. Biol. Chem. 274, 10086 (1999).

22. Nakajima, Y. et al. A relationship between protein kinase C phosphorylation and calmodulin binding to the metabotropic glutamate receptor subtype 7. J. Biol. Chem. 274, 27573 (1999).

23. Leonard, A. S. et al. Regulation of calcium/calmodulin-dependent protein kinase II docking to N-methyl-D-aspartate receptors by calcium/calmodulin and alpha-actinin. J. Biol. Chem. 277, 48441 (2002).

24. McCullar, J. S. et al. Calmodulin is a phospholipase C-beta interacting protein. J. Biol. Chem. 278, 33708 (2003).

25. Klee, C. B. et al. Calcineurin: a calcium- and calmodulin-binding protein of the nervous system. Proc. Natl. Acad. Sci. U. S. A. 76, 6270 (1980).

26. Sheng, M. et al. CREB: a $Ca^{(2+)}$-regulated transcription factor phosphorylated by calmodulin-dependent kinases. Science. 252, 1427 (1991).

27. Yokoyama, C. T. et al. Phosphorylation of the synaptic protein interaction site on N-type calcium channels inhibits interactions with SNARE proteins. J. Neurosci. 17, 6929 (1997).

28. Fukunaga, K. et al. Decreased protein phosphatase 2A activity in hippocampal long-term potentiation. J. Neurochem. 74, 807 (2000).

29. Enslen, H. et al. Characterization of Ca^{2+}/calmodulin-dependent protein kinase IV. Role in transcriptional regulation. J. Biol. Chem. 269, 15520 (1994).

30. Sun, Z. et al. Calspermin gene transcription is regulated by two cyclic AMP response elements contained in an alternative promoter in the calmodulin kinase IV gene. Mol. Cell. Biol. 15, 561 (1995).

31. Yano, S. et al. Calcium promotes cell survival through CaM-K kinase activation of the protein-kinase-B pathway. Nature. 396, 584 (1999).

32. Edelman, A. M. et al. Multiple $Ca^{(2+)}$-calmodulin-dependent protein kinase kinases from rat brain. Purification, regulation by $Ca^{(2+)}$-calmodulin, and partial amino acid sequence. J. Biol. Chem. 271, 10806 (1996).

33. Madison, D. V. et al. Phorbol esters block a voltage-sensitive chloride current in hippocampal pyramidal cells. Nature. 321, 695 (1986).

34. Bannister, A. J. et al. Stimulation of c-Jun activity by CBP: c-Jun residues Ser63/73 are required for CBP induced stimulation in vivo and CBP binding in vitro. Oncogene. 11, 2509 (1996).

35. Hai, T. & Curran, T. Cross-family dimerization of transcription factors Fos/Jun and ATF/CREB alters DNA binding specificity. Proc. Natl. Acad. Sci. U. S. A. 88, 3720 (1991).

36. Foulkes, N. S. et al. CREM gene: use of alternative DNA-binding domains generates multiple antagonists of cAMP-induced transcription. Cell. 64, 739 (1991).

37. Sidhu, A. et al. D1 dopamine receptors can interact with both stimulatory and inhibitory guanine nucleotide binding proteins. J. Neurochem. 57, 1445 (1991).

38. Grilli, M. et al. Pharmacological characterization of D1 and D2 dopamine receptors in rat limbocortical areas. II. Dorsal hippocampus. Neurosci. Lett. 87, 253 (1988).

39. Obadiah, J. et al. Adenylyl cyclase interaction with the D2 dopamine receptor family; differential coupling to Gi, Gz, and Gs. Cell. Mol. Neurobiol. 19, 653 (1999).

40. Yang, M. et al. Requirement of Gbetagamma and c-Src in D2 dopamine receptor-mediated nuclear factor-kappaB activation. Mol. Pharmacol. 64, 447 (2003).

41. Beom, S. et al. Comparative studies of molecular mechanisms of dopamine D2 and D3 receptors for the activation of extracellular signal-regulated kinase. J. Biol. Chem. 279, 28304 (2004).

42. Oldenhof, J. et al. SH3 ligands in the dopamine D3 receptor. Cell. Signal. 13, 411 (2001).

43. Taussig, R. et al. Inhibition of adenylyl cyclase by Gi alpha. Science. 261, 218 (1993).

44. Ross, E. M. et al. Reconstitution of hormone-sensitive adenylate cyclase activity with resolved components of the enzyme. J. Biol. Chem. 253, 6401 (1978).

45. Dessauer, C. W. et al. Identification of a Gialpha binding site on type V adenylyl cyclase. J. Biol. Chem. 273, 25831 (1998).

46. Kozasa, T. & Gilman, A. G. Purification of recombinant G proteins from Sf9 cells by hexahistidine tagging of associated subunits. Characterization of alpha 12 and inhibition of adenylyl cyclase by alpha z. J. Biol. Chem. 270, 1734 (1995).

47. Tang, W. J. & Gilman, A. G. Type-specific regulation of adenylyl cyclase by G protein beta gamma subunits. Science. 254, 1500 (1992).

48. De Waard, M. et al. Direct binding of G-protein betagamma complex to voltage-dependent calcium channels. Nature. 385, 446 (1997).

49. Stephens, L. et al. A novel phosphoinositide 3 kinase activity in myeloidderived cells is activated by G protein beta gamma subunits. Cell. 77, 83 (1994).

50. Camps, M. et al. Isozyme-selective stimulation of phospholipase C-beta 2 by G protein beta gamma-subunits. Nature. 360, 684 (1993).

51. Xu, N. et al. The PH domain of Ras-GAP is sufficient for in vitro binding to beta gamma subunits of heterotrimeric G proteins. Cell. Mol. Neurobiol. 16, 51 (1996).

52. Sugiyama, H. et al. Glutamate receptor subtypes may be classified into two major categories: a study on Xenopus oocytes injected with rat brain mRNA. Neuron. 3, 129 (1990).

53. Harris, S. L. & Levine, A. J. The p53 pathway: Positive and negative feedback loops. Oncogene. 24, 2899 (2005).

54. Najib, S. & Sanchez-Margalet, V. Sam68 associates with the SH3 domains of Grb2 recruiting GAP to the Grb2-SOS complex in insulin receptor signaling. J. Cell. Biochem. 86, 99 (2002).

55. Wei, W. et al. The v-Jun point mutation allows c-Jun to escape GSK3-dependent recognition and destruction by the Fbw7 ubiquitin ligase. Cancer. Cell. 8, 25 (2005).

56. Fiol, C. J. et al. A secondary phosphorylation of CREB341 at Ser129 is required for the cAMP-mediated control of gene expression. A role for glycogen synthase kinase-3 in the control of gene expression. J. Biol. Chem. 269, 32187 (1995).

57. Delcommenne, M. et al. Phosphoinositide-3-OH kinase-dependent regulation of glycogen synthase kinase 3 and protein kinase B/AKT by the integrinlinked kinase. Proc. Natl. Acad. Sci. U. S. A. 95, 11211 (1998).

58. Crespo, P. et al. Ras-dependent activation of MAP kinase pathway mediated by G-protein beta gamma subunits. Nature. 369, 418 (1994).

59. Yan, Z. & Surmeier, D. J. Muscarinic (m2/m4) receptors reduce N- and Ptype Ca^{2+} currents in rat neostriatal cholinergic interneurons through a fast, membrane-delimited, G-protein pathway. J. Neurosci. 16, 2592 (1996).

60. Masu, M. et al. Sequence and expression of a metabotropic glutamate receptor. Nature. 349, 760 (1991).

61. MacDermott, A. B. et al. NMDA-receptor activation increases cytoplasmic calcium concentration in cultured spinal cord neurones. Nature. 321, 519 (1986).

62. Gurd, J. W. & Bissoon, N. The N-methyl-D-aspartate receptor subunits NR2A and NR2B bind to the SH2 domains of phospholipase C-gamma. J. Neurochem. 69, 623 (1997).

63. Westenbroek, R. E. et al. Biochemical properties and subcellular distribution of an N-type calcium channel alpha 1 subunit. Neuron. 9, 1099 (1993).

64. Hillman, D. et al. Localization of P-type calcium channels in the central nervous system. Proc. Natl. Acad. Sci. U. S. A. 88, 7076 (1991).

65. Alessi, D. R. et al. Characterization of a 3-phosphoinositide-dependent protein kinase which phosphorylates and activates protein kinase Balpha. Curr. Biol. 7, 261 (1997).

66. Dutil, E. M. et al. Regulation of conventional protein kinase C isozymes by phosphoinositide-dependent kinase 1 (PDK-1). Curr. Biol. 8, 1366 (1999).

67. Jensen, C. J. et al. 90-kDa ribosomal S6 kinase is phosphorylated and activated by 3-phosphoinositide-dependent protein kinase-1. J. Biol. Chem. 274, 27168 (1999).

68. Whitman, M. et al. Type I phosphatidylinositol kinase makes a novel inositol phospholipid, phosphatidylinositol-3-phosphate. Nature. 332, 644 (1988).

69. Stephens, L. et al. Protein kinase B kinases that mediate phosphatidylinositol 3,4,5-trisphosphate-dependent activation of protein kinase B. Science. 279, 710 (1998).

70. Singh, S. S. et al. Activation of protein kinase C by phosphatidylinositol 3,4,5-trisphosphate. Biochem. Biophys. Res. Commun. 195, 104 (1993).

71. Constantinescu, A. et al. cAMP-dependent protein kinase type I regulates ethanol-induced cAMP response element-mediated gene expression via activation of CREB-binding protein and inhibition of MAPK. J. Biol. Chem. 279, 43321 (2004).

72. Montminy, M. R. et al. Identification of a cyclic-AMP-responsive element within the rat somatostatin gene. Proc. Natl. Acad. Sci. U. S. A. 83, 6682 (1986).

73. Zamanillo, D. et al. Identification of a cyclic adenosine 3',5'-monophosphatedependent protein kinase phosphorylation site in the carboxy terminal tail of human D1 dopamine receptor. Neurosci. Lett. 188, 183 (1995).

74. Sorensen, S. D. et al. Dissociation of protein kinase-mediated regulation of metabotropic glutamate receptor 7 (mGluR7) interactions with calmodulin and regulation of mGluR7 function. Mol. Pharmacol. 61, 1303 (2002).

75. Leonard, A. S. & Hell, J. W. Cyclic AMP-dependent protein kinase and protein kinase C phosphorylate N-methyl-D-aspartate receptors at different sites. J. Biol. Chem. 272, 12107 (1997).

76. Wu, L. et al. Dual regulation of voltage-gated calcium channels by PtdIns(4,5)P2. Nature. 419, 947 (2002).

77. Liu, M. & Simon, M. I. Regulation by cAMP-dependent protein kinase of a G-protein-mediated phospholipase C. Nature. 382, 83 (1996).

78. Kim, U. H. et al. Phosphorylation of phospholipase C-gamma by cAMPdependent protein kinase. J. Biol. Chem. 264, 20167 (1990).

79. Yoshimura, M. & Cooper, D. M. Type-specific stimulation of adenylylcyclase by protein kinase C. J. Biol. Chem. 268, 4604 (1993).

80. Kawabe, J. et al. Differential activation of adenylyl cyclase by protein kinase C isoenzymes. J. Biol. Chem. 269, 16554 (1994).

81. Goode, N. et al. Differential regulation of glycogen synthase kinase-3 beta by protein kinase C isotypes. J. Biol. Chem. 267, 16878 (1992).

82. Sato, M. et al. Altered agonist sensitivity and desensitization of neuronal mGluR1 responses in knock-in mice by a single amino acid substitution at the PKC phosphorylation site. Eur. J. Neurosci. 20, 947 (2004).

83. Tingley, W. G. et al. Regulation of NMDA receptor phosphorylation by alternative splicing of the C-terminal domain. Nature. 364, 70 (1993).

84. Swartz, K. J. et al. Protein kinase C modulates glutamate receptor inhibition of Ca^{2+} channels and synaptic transmission. Nature. 361, 165 (1993).

85. Litosch, I. Protein kinase C inhibits the Ca(2+)-dependent stimulation of phospholipase C-beta 1 in vitro. Recept. Signal. Transduct. 6, 87 (1997).

86. Burgess, G. M. et al. The second messenger linking receptor activation to internal Ca release in liver. Nature. 309, 63 (1984).

87. Runnels, L. W. et al. The TRPM7 channel is inactivated by PIP(2) hydrolysis. Nat. Cell. Biol. 4, 329 (2002).

88. Stahl, M. L. et al. Sequence similarity of phospholipase C with the noncatalytic region of src. Nature. 332, 269 (1988).

89. Meisenhelder, J. et al. Phospholipase C-gamma is a substrate for the PDGF and EGF receptor protein-tyrosine kinases in vivo and in vitro. Cell. 57, 1109 (1989).

90. Mora, A. et al. Lithium blocks the PKB and GSK3 dephosphorylation induced by ceramide through protein phosphatase-2A. Cell. Signal. 14, 557 (2002).

91. DeRemer, M. F. et al. Ca(2+)-calmodulin-dependent protein kinases Ia and Ib from rat brain. II. Enzymatic characteristics and regulation of activities by phosphorylation and dephosphorylation. J. Biol. Chem. 267, 13466 (1992).

92. Westphal, R. S. et al. A signaling complex of Ca^{2+}-calmodulin-dependent protein kinase IV and protein phosphatase 2A. Science. 280, 1258 (1998).

93. Wadzinski, B. E. et al. Nuclear protein phosphatase 2A dephosphorylates protein kinase A-phosphorylated CREB and regulates CREB transcriptional stimulation. Mol. Cell. Biol. 13, 2822 (1993).

94. Wang, L. Y. et al. Regulation of NMDA receptors in cultured hippocampal neurons by protein phosphatases 1 and 2A. Nature. 369, 230 (1994).

95. Kasahara, J. et al. Differential effects of a calcineurin inhibitor on glutamateinduced phosphorylation of Ca^{2+}/calmodulin-dependent protein kinases in cultured rat hippocampal neurons. J. Biol. Chem. 274, 9061 (1999).

96. Lieberman, D. N. & Mody, I. Regulation of NMDA channel function by endogenous Ca(2+)-dependent phosphatase. Nature. 369, 235 (1994).

97. Yue, Y. et al. Ras GTPase-activating protein binds to Akt and is required for its activation. J. Biol. Chem. 279, 12883 (2004).

98. Xing, J. et al. Coupling of the RAS-MAPK pathway to gene activation by RSK2, a growth factor-regulated CREB kinase. Science. 273, 959 (1996).

99. Hong, W. et al. Physical and functional interaction between the transcriptional cofactor CBP and the KH domain protein Sam68. Mol. Cancer. Res. 1, 48 (2002).

100. Kobilka, B. K. et al. An intronless gene encoding a potential member of the family of receptors coupled to guanine nucleotide regulatory proteins. Nature. 329, 75 (1987).